

Architecture of turbidite channel systems on the continental slope: Patterns and predictions

T. McHargue^{a,*}, M.J. Pyrcz^b, M.D. Sullivan^b, J.D. Clark^a, A. Fildani^a, B.W. Romans^a, J.A. Covault^a, M. Levy^a, H.W. Posamentier^b, N.J. Drinkwater^c

^aChevron Energy Technology Company, 6001 Bollinger Canyon Road, San Ramon, CA, USA

^bChevron Energy Technology Company, Houston, TX, USA

^cChevron South African Business Unit, Houston, TX, USA

ARTICLE INFO

Article history:

Received 16 January 2010

Received in revised form

11 July 2010

Accepted 14 July 2010

Available online 29 July 2010

Keywords:

Turbidite

Turbidite architecture

Turbidite channel

Continental slope

Cyclicality

Modeling

Petroleum reservoir

Process

Turbidity current

ABSTRACT

The study of many slope channel systems has led to the development of rules in the form of observations, measurements, and hypotheses. For example, we hypothesize that high abandonment relief can strongly influence the location of the subsequent channel element and will result in an organized channel stacking pattern in which the path of the younger channel element approximates the path of the former element. The rules were developed with the objective of constructing forward models of petroleum reservoirs that are internally consistent, reproducible, and quantifiable. Channelized turbidite deposits can be interpreted to be the product of multiple cycles of waxing–waning flow energy at multiple scales. Systematic changes in the volume and caliber of turbidity flows through time trigger a fall of the equilibrium profile, which drives erosion and sediment bypass across the slope, followed by a rise of the equilibrium profile, which allows deposition on the slope of increasingly mud-rich sediments through time. In most turbidite successions, at least three scales of waxing–waning cyclicality can be interpreted: element, complex set, and sequence. The stacking pattern of channel elements within a complex set-scale cycle tends to be sequential: (1) erosion and sediment bypass; (2) amalgamation of channel elements associated with a low rate of aggradation; (3) a disorganized stacking pattern of channel elements associated with a moderate rate of aggradation; and (4) an organized stacking pattern of channel elements associated with a high rate of aggradation. Stages 1 and 2 may be absent or minor in mud-rich systems but prominent in sand-rich systems. Conversely, stage 4 may be prominent in mud-rich systems but absent in sand-rich systems. Event-based forward modeling, utilizing rules, can produce realistic architectures, such as the four stages described above. Multiple realizations and multiple alternative models can be constructed to quantitatively examine the probability of specific parameters of interest such as pore volume and connectivity.

© 2010 Elsevier Ltd. All rights reserved.

1. Introduction

Turbidite channel systems are a common type of sandstone deposit on the continental slope and have proven to be one of the most common types of hydrocarbon reservoirs found in deep ocean settings (Weimer et al., 2000). Despite their abundance and many years of study, both in industry and academia, characterization and predictability have proven challenging due to the three-dimensional complexity and diversity of channel systems. The petroleum industry is interested in improved characterization of turbidite

channel systems, because of the high cost of discovering and extracting oil and gas from these complicated reservoirs in deep-water, far offshore. Complexity yields significant degrees of uncertainty as to the volume of hydrocarbons in place, the volume of hydrocarbons that are likely to be recovered during production, and the scale of facilities needed to most efficiently recover the hydrocarbons. In such a challenging and expensive setting, it is highly advantageous to be able to reduce uncertainty to a minimum and to accurately define the range of the uncertainty that remains.

Magallanes Basin outcropping strata serve as the inspiration of the Special Issue in which this manuscript is published. The basin hosts three distinct formations, each of which displays a characteristic deep-water architecture in exceptionally well exposed outcrops (Fildani et al., 2009). The factors that may control the observed changes in stratigraphic architecture were discussed

* Corresponding author. Present address: Stanford University, Department of Geological and Environmental Sciences, Stanford, CA 94305-2115, USA. Tel.: +1 925 964 0740.

E-mail address: timchar@stanford.edu (T. McHargue).

during the 2009 SEPM Field Conference. Such exceptionally well exposed outcrop examples of ancient systems (e.g., Bernhardt et al., 2011; Fildani et al., 2009; Flint et al., 2011; Hubbard et al., 2010; Kane and Hodgson, 2011; Khan and Arnott, 2011; Romans et al., 2011) are sources of data that contribute significantly to our understanding of turbidite channel systems. Other important sources include oceanographic data from “modern” systems, near surface 2D and 3D seismic surveys (both high resolution and industry standard) (e.g., Posamentier and Kolla, 2003), and subsurface data from ancient systems (core, well logs, bore-hole images, pressure data, fluid production, etc.). What is lacking for turbidite systems that usually are available for other depositional systems are direct observations of on-going processes of erosion and deposition. Consequently, processes are poorly understood and are based on the study of synthetic systems in flume tanks and numerical models of flow mechanics. This “process gap” in our knowledge of turbidites is a major handicap. Until recently, the most valuable sources of information regarding turbidite channel architectures have been outcrops, especially exceptionally well exposed, aerially extensive outcrops. Unfortunately, there are few of these exceptional outcrop exposures. They tend to be biased in favor of very sand-rich deposits in epicratonic settings, and essentially are two-dimensional or, at best, consist of a set of two-dimensional exposures (Campion et al., 2000; Gardner and Borer, 2000; Sullivan et al., 2000; Fildani et al., 2009; Hubbard et al., 2010; Pyles et al., 2010). More recently, high quality 3D seismic-reflection surveys have yielded many vivid 3D images of turbidite channel systems from continental margin settings around the world (e.g., Weimer et al., 2000; Posamentier and Kolla, 2003). Architecture is revealed at a coarse scale relative to outcrop exposures, and samples of lithologies within the revealed architectures usually are lacking. Despite these limitations, 3D seismic-reflection surveys provide the only robust three-dimensional constraints on architectural complexity and evolution through time and space. The lack of lithological control is mitigated somewhat by internally consistent displays of the variation in reflection attributes, such as amplitudes, throughout the 3D space. When available, well data provide lithological calibration for attribute displays and help to constrain interpretations of lithologies away from the well bores. Ultimately, all sources of information regarding turbidite channels have both strengths and weaknesses, so a robust understanding of these complicated systems is most likely to result from the integration of data from all sources.

Conceptual models of turbidite channel architecture have been developed to summarize the characteristics of specific outcrops or subsurface examples (e.g., Stelting et al., 1985; Phillips, 1987; Mutti, 1985; McHargue, 1991; Pirmez and Flood, 1995; Clark and Pickering, 1996; Gardner and Borer, 2000; Mayall and Stewart, 2000; Navarre et al., 2002). These models are intended to serve as a basis for making predictions about the characteristics of a poorly known example, such as a subsurface reservoir. Traditionally conceptual models have been conveyed as 2D profiles or 3D block diagrams. These diagrams, and the studies on which they are based, remain important analogs that guide predictions and constrain uncertainty. However, each of them can suffer from being too specific to a narrow set of conditions. If the conditions for a subsurface reservoir differ from the analog, then predictions based on that single analog are unlikely to be correct for the reservoir and the uncertainty around that error is unknown. On the other hand, general models that attempt to synthesize observations from many examples have tended to be fairly vague with simplified architectures that lack sufficient detail at the reservoir scale (Mitchum, 1984, 1985; Mutti, 1985; Posamentier and Vail, 1988; Reading and Richards, 1994; Clark and Pickering, 1996; Prather

et al., 1998). Reservoir scale predictions based on these general models also tend to yield a high degree of uncertainty.

An emerging approach is to construct quantitative forward models that replicate the known characteristics (i.e., conditioning data) of a reservoir and predict the range and probability of possible unknown characteristics that are compatible with the conditioning data (Pyrzcz, 2004; Pyrcz et al., in press; Sylvester et al., 2011). Forward models can be constructed in several different ways, based on the assumptions that the modelers are comfortable with making. To date, all forward modeling schemes require numerous assumptions. One of these approaches, event-based modeling (Pyrzcz, 2004; Pyrcz and Deutsch, 2005; Pyrcz et al., 2005; Pyrcz et al., 2006; Pyrcz and Strebelle, 2006; Pyrcz et al., in press; McHargue et al., in press), is a rule-based approach and is addressed in this paper by discussing the geologic concepts behind some of the rules and illustrating example products of these models.

2. Classification hierarchy

It is essential to organize and synthesize observations by hierarchical scale into recurring patterns, trends, or statistical distributions which we refer to as rules. Some rules may apply to multiple hierarchical scales, but more likely, they do not, so it is necessary to correlate rules with the hierarchical scale to which they apply. Several hierarchical schemes for turbidite channel systems have been proposed (e.g. Campion et al., 2000; Gardner and Borer, 2000; Navarre et al., 2002; Sprague et al., 2002, 2005). The scheme used here most closely resembles that of Sprague et al. (2002, 2005). Although some of the terms used here are modified from Sprague et al., the conceptual basis remains the same. This hierarchical scheme is designed to be applicable to 1D and 2D data and can be problematic in three dimensions.

In channelized systems, the fundamental architectural unit is the channel element, which consists of a channel-form surface and the sediments that fill it (Fig. 1). Separate elements are distinguished from each other by an abrupt lateral offset of depositional facies. Temporal duration and physical scale do not contribute to the definition. Individual channel elements may consist of multiple smaller channel-forms, called stories, which essentially stack vertically with no significant lateral offset of depositional facies. Multiple similar and genetically related elements that stack in a consistent pattern constitute a single complex. If multiple genetically related complexes are present, they form a single complex set. The term system is a general term used to refer to all of the genetically related erosional and depositional components that are present in a single area regardless of hierarchy. A system is most often equivalent to one or more complex sets or, less commonly, to a complex. In sequence stratigraphic terms, the lowstand system tract of a 3rd order sequence often will consist of multiple complex sets. A single complex set might represent the lowstand portion of a single high frequency sequence.

3. Element lithofacies patterns

The sediments that fill channel elements usually can be organized into a predictable pattern of facies associations; axis, off-axis, and margin (Fig. 1). In a relative sense, these facies associations differ from each other by the degree of amalgamation of beds and the relative abundance of sand. Of the three facies associations, the axis is located at the thickest part of the channel element, displays the greatest amount of amalgamation, has the thickest beds, and has the highest concentration of sand. In contrast, the margin facies association is located at the thinner parts of the channel element, displays the least amalgamation, has the thinnest beds, and has the lowest concentration of sand. The off-axis facies association has

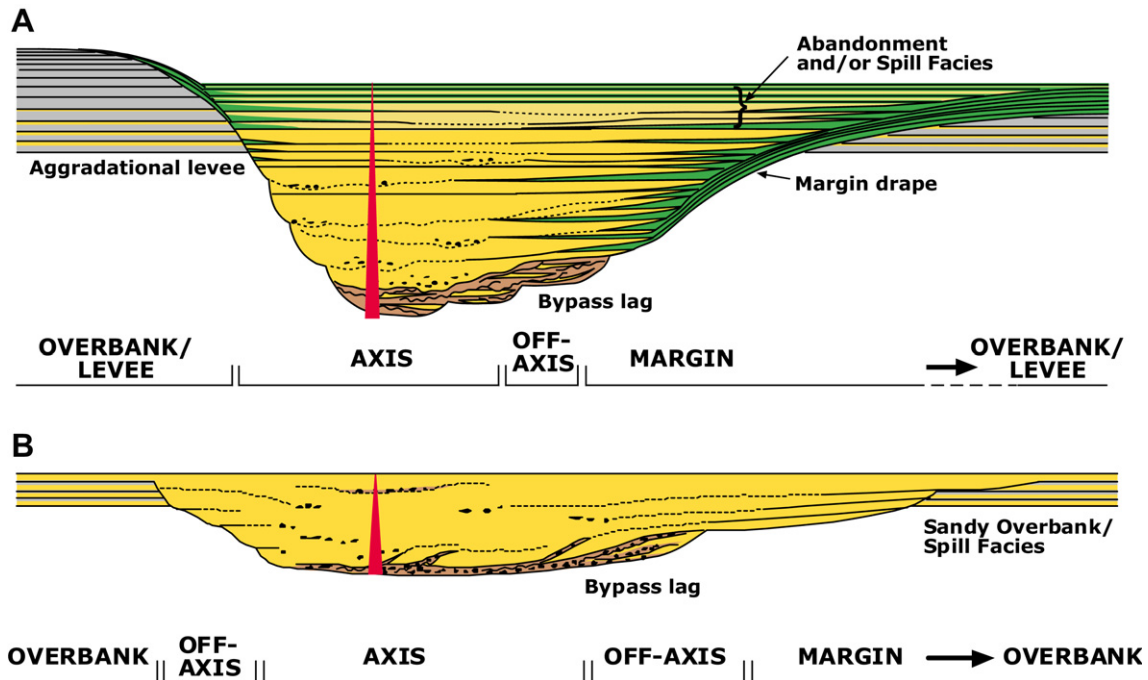


Fig. 1. Schematic representations of common fill styles of under-filled and filled channel elements. Although the contrasting characteristics as illustrated here are common for these two channel types, variation is considerable. A: Under-filled channel element with moderate to high rate of overbank aggradation, semi-amalgamated highly heterolithic fill, common shale/silt drapes, and capped by upward fining abandonment-fill facies. B: Filled channel element with low rate of overbank aggradation, amalgamated and less heterolithic fill, and rare shale/silt drapes. Upward fining abandonment-fill facies is thin or absent. If the channel element is over-filled, sandy overbank deposits may be present. Yellow = sand-rich channel-fill sediments, Green = mud-rich channel-fill sediments, Brown = mud-clast-rich channel-fill sediments, Gray = mud-rich pre-existing sediments.

characteristics that are intermediate between the other two facies associations. Because some channel elements are sandy high energy features and others are much muddier, the channel-fill facies associations are not defined by specific values of sand percentage or bed thickness, but by the relative trend of these values within a channel element.

Vertical trends of sand percentage or bed thickness within a single element also may be helpful for identifying which channel-fill facies association is present at a particular location (Fig. 1). The axis facies association, because of abundant amalgamation, tends to have a blocky-shaped sandy grain-size profile with minor mudstone interbeds. However, mudstone in the form of mass flow deposits or thick shale-clast lag deposits often is present or even abundant in the axis facies association and can cause considerable complications in the appearance of the vertical profile. In the channel margin facies association, both sand abundance and bed thicknesses tend to increase upward and mudstone interbeds are common. Mass flow deposits and shale-clast lag deposits may be present in the margin facies association, but usually they are less common in the margin than in the axis of the channel element. The off-axis facies association has intermediate characteristics between the axis and the margin facies associations.

A fourth channel-fill facies association, the abandonment facies association, is present in many, but not all, channel elements (Fig. 1). If present, it overlies all of the other channel-fill facies associations. In the channel abandonment facies association, both sand abundance and bed thickness tend to decrease upward and mudstone interbeds are common (Labourdet, 2007). Above the underlying axis facies association, the abandonment facies association tends to be relatively sandy and amalgamated compared to the abandonment deposits that underlie the channel margin facies association (Fig. 1).

Cross-sections of single channel elements can be symmetrical or asymmetrical. In high resolution 3D seismic volumes and in high

resolution bathymetric images of modern channels on the ocean bottom, symmetrical channels have been noted at the straight segments of channel elements, whereas asymmetrical elements are found at sinuous channel bends with the thickest part of the element displaced toward the outer bend (Abreu et al., 2003; Posamentier and Kolla, 2003; Deptuck et al., 2007). Likewise, the axis facies association is located at the thick center of symmetrical channels and is displaced from the center toward the thicker, outer portion of asymmetrical channel elements (Pyles et al., 2010). Accordingly, off-axis and margin facies associations may expand in width on the inner, thinner side of asymmetrical channel elements and be narrow or absent at the outer, thicker side of the channel element. The magnitude of asymmetry in channel elements is thought to be proportional to the magnitude of sinuosity (e.g. Gardner and Borer, 2000; Peakall et al., 2000; Abreu et al., 2003; Pyles et al., 2010), but robust documentation and quantification of this relationship is lacking.

4. Channel dimensions

Although channel elements are not defined based on their dimensions, some patterns have been detected that might prove instructive for interpreting the depositional setting of isolated outcrops or well penetrations of channel elements. When building models in the absence of sufficient local information, the data compiled in Fig. 2 can be used as a guide to size distributions of channel elements.

Element dimensions from any confined channelized system, whether levee-confined or erosionally confined, are included in Fig. 2. Likewise, data are included in Fig. 2 regardless of sand/mud ratio or paleo-seafloor gradient. Channel element dimensions measured from outcrops and subsurface data have been compiled from the literature, supplemented with proprietary data collected

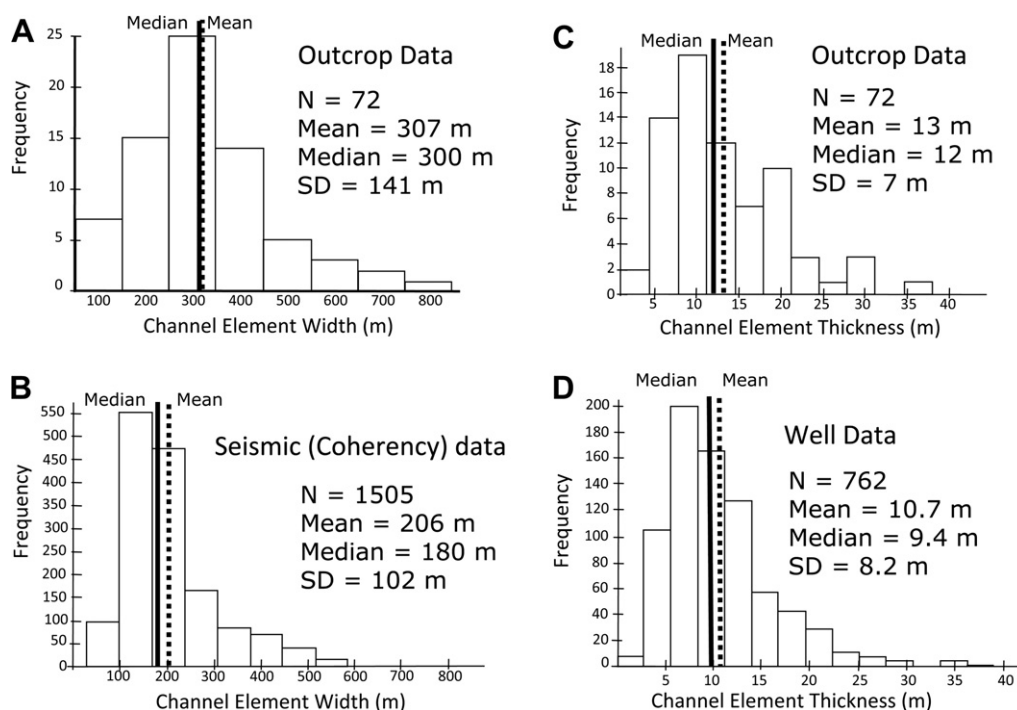


Fig. 2. Histograms of measured channel element widths and thicknesses. SD = standard deviation. N = number of measured examples. A: Histogram of channel element widths from outcrop examples. B: Histogram of channel element widths from high quality 3D reflection seismic coherency data. C: Histogram of channel element thicknesses from outcrop examples. D: Histogram of channel element thicknesses from well logs (only penetrations through axis facies association).

by the authors. Only channel elements with the most complete dimensions were included in Fig. 2.

4.1. Channel width

Good quality 3D seismic data provide an excellent opportunity to measure the widths of many channel elements in multiple locations. These measurements demonstrate that the widths of channel elements typically fall between 100 and 300 m with an average of 206 m (Fig. 2). Measurements from outcrops suggest a wider range of values for channel element width with an average of 307 m (Fig. 2). The different results for the two data sets are not understood, but it is likely related to the following potential weaknesses of the data sources. Because vertical resolution is poor in most conventional 3D seismic data sets relative to the thickness of channel elements, many elements fall within a single seismic wavelength. Therefore, seismic-based measurements of element width may represent an average value between a maximum value at the top of the channel element and a minimum value at the base. Channel element width measurements from outcrops are also potentially biased toward an overestimate of element widths because outcrops rarely are perpendicular to the flow direction of the channel element. Therefore, element widths measured from outcrops generally are apparent widths that need to be corrected. Although the correction is routinely attempted, the correction is always subject to error. Other uncertainties result from mixing measurements from multiple hierarchical levels. For example, the often cited compilation of channel dimensions in Clark and Pickering (1996) contains no hierarchical information. For the compilation in Fig. 2, data from the literature were hierarchically classified by the authors.

4.2. Channel thickness

As discussed, even good quality 3D seismic data rarely provide the opportunity to collect robust measurements of channel element

thicknesses because of inadequate resolution. Fortunately, high quality outcrops can be well suited for providing accurate element thicknesses (Clark and Pickering, 1996) and provide our best source for channel thickness data (Fig. 2C). Nevertheless, channel thickness measurements from outcrops can have significant errors. For example, sediments that fill the top of channel elements often are muddy (Figueiredo et al., 2010; Flint et al., 2011) and may be poorly exposed. This issue may lead to a significant underestimate of channel element thickness. Also, amalgamation of multiple sand-rich elements may make the base of some elements indistinct. As mentioned above, other uncertainties result from imperfect exposure or incomplete published information as to what hierarchical level is being measured. Wells also can be a useful source of data regarding channel element thicknesses. However, like outcrop data sets, amalgamation is a common source of uncertainty. Many channel elements are thinned due to erosion by younger elements. Furthermore, many wells penetrate the channel element at a location that is less than its maximum thickness. Channel element thicknesses from well data are included in Fig. 2D only if the well penetrated an uneroded element through the axial facies association. Outcrop examples yield a mean of 13 m whereas well data yield a mean of 10.7 m for channel element thickness (Fig. 2).

We hypothesize that the thickness of a channel element is related to depositional setting; either proximal vs. distal or, more likely, high gradient vs. low gradient. Documentation to support the relationship between channel element thickness and depositional gradient is weak, because the interpretation of depositional gradient is subjective for ancient examples.

5. Gradient patterns

5.1. Depth of erosion

Gradient influences turbidite channel architecture by contributing to the force of turbidity flows; force is proportional to the

steepness of the gradient. The first order effect of gradient on architecture is its influence on the depth of erosion. For a given channel element, all else being equal, erosional depth is greatest where the gradient is steepest (Pirmez et al., 2000; Prather et al., 2000; Ferry et al., 2005). If channel element thickness is controlled solely by erosion, then element thickness would be a good approximation of slope gradient. This is most likely to be true for sand-rich systems which generally lack appreciable overbank development (Mutti, 1985; Mutti and Normark, 1987). But for muddy systems, overbank aggradation also contributes significantly to the thickness of channel elements and, on a local scale, the thickness of overbank aggradation may not correlate well with gradient (Pirmez and Imran, 2003).

5.2. Accommodation

An equilibrium profile in turbidite channels, as in fluvial systems, is the theoretical elevation along the path of the channel at which there is no net erosion or deposition (Pirmez et al., 2000; Kneller, 2003). The height of the equilibrium profile above the sediment surface at any point along the equilibrium profile represents the thickness of accommodation at that point in time (Posamentier and Vail, 1988; Samuel et al., 2003). The gradient of the equilibrium profile develops in response to changes in flow height, density, and grain size. Larger, sandier flows trigger a decrease in the equilibrium gradient and, therefore, a decrease in accommodation whereas smaller, muddier flows trigger an increase in the equilibrium gradient and an increase in accommodation (Kneller, 2003). Over long periods of time, accommodation at any point along a channel profile changes substantially, but change tends to follow a pattern in most channel systems: erosion, to some degree, early in the history of the channel system followed by deposition and aggradation late in the history of the system (Stelting et al., 1985; McHargue, 1991; Peakall et al., 2000; Deptuck et al., 2003; Kneller, 2003; Labourdette, 2007). Although the longitudinal profile of entire channel systems often is concave (Pirmez et al., 2000; Pirmez and Imran, 2003), the longitudinal profile of many turbidite channel systems on the slope is nearly linear for several tens of kilometers (Fig. 3). Furthermore, despite substantial changes in accommodation history, the gradient of the longitudinal profile of many turbidite channel systems appears to remain fairly constant through time. This pattern is illustrated by a near modern turbidite channel system offshore Nigeria, where the base of the erosional turbidite channel system is nearly linear for 60 km, as interpreted from excellent quality 3D seismic data (Fig. 4). Likewise, at the time the system was abandoned, the top of channel-fill and the tops of levees also constructed a smooth, linear, longitudinal bathymetric profile, approximately parallel to the original, erosional profile at the base of the system (Fig. 4). Apparently, the gradient of the equilibrium profile changed little with time and a single accommodation history can reasonably be applied to this entire channel segment. This is an important simplifying assumption for constructing a forward model of this type of turbidite channel system.

Although it has not been demonstrated, we assume for modeling purposes that the apparently constant gradient of the equilibrium profile for several tens of kilometers applies to element-scale architecture as well as to complex and complex set-scale architecture. So, for channel segments that are a few tens of kilometers long, it is assumed that a single accommodation cycle reasonably predicts erosion and then fill of a channel element at all points along the entire length of the channel segment. Multiple elements result from multiple accommodation cycles of similar scale.

On the other hand, if adjacent channel elements with very different depths of erosion are present in the same system, then equilibrium disruption (Pirmez et al., 2000) is indicated with

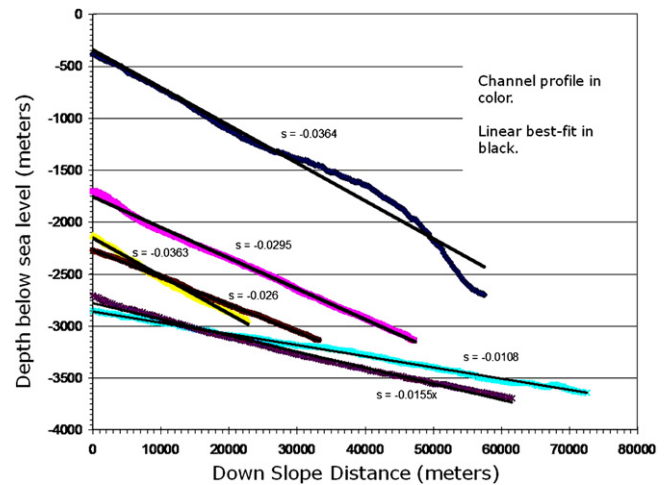


Fig. 3. Example bathymetric profiles (colored lines) from the continental slope of the Niger Delta showing thalweg elevations of six channel systems near the seafloor that are well imaged by 3D reflection seismic surveys. In all but one of the examples, straight lines (black) closely approximate the thalweg profiles. These examples demonstrate that, although gradients differ for separate channel systems, most channel systems are well approximated by assuming a constant equilibrium gradient for distances of several tens of kilometers down the slope. Therefore, it is reasonable to assume that channel gradient was nearly constant for a channel element for distances greater than expected for a single hydrocarbon accumulation. Examples where a constant channel gradient is an inappropriate approximation (i.e. the shallowest example illustrated here) can be anticipated because isochron thicknesses will vary along the flow path in these instances.

substantial changes in the gradient of the profile of one element relative to the other. Equilibrium disruption results either from dramatic differences in the evolution of flow characteristics or from topographic irregularities along the flow path that are either too great or too dynamic to have been smoothed by erosion (e.g. the shallowest example in Fig. 3). Examples include ponded or fill-and-spill systems (Winker, 1996; Prather et al., 1998; Beaubouef and Friedman, 2000; Pirmez et al., 2000; Mayall and Stewart, 2001) and transient fans (Adeogba et al., 2005). Although systems like these can be important hydrocarbon reservoirs, the simplifying assumptions described in the previous paragraph are inappropriate for modeling them.

6. Cyclicity patterns

6.1. Waxing–waning cycle

A cycle of channel erosion followed by deposition of channel-filling sediments has long been recognized (Mutti and Normark, 1987, 1991). Building on this recognition, we find it useful to interpret channelized turbidite deposits to be the product of multiple cycles of waxing flow energy followed by waning flow energy at multiple scales. Each cycle is interpreted to result from systematic, and presumably gradual, changes in the volume and caliber of turbidity flows through time triggering first a fall and then a rise of the equilibrium profile (Kneller, 2003). In the waxing portion of an energy cycle, flows are relatively large and dense, and sediment caliber usually is coarse (sand-rich) relative to flows of the waning phase. Therefore, the waxing phase of the cycle drives erosion of a channel conduit as the equilibrium profile falls. Eventually, successive flows gradually decrease in force; the equilibrium profile stabilizes and then begins to rise. The rise of the equilibrium profile marks the beginning of the waning phase of the energy cycle. As the equilibrium profile rises in the waning phase, flows progressively become smaller, and usually muddier in caliber, with

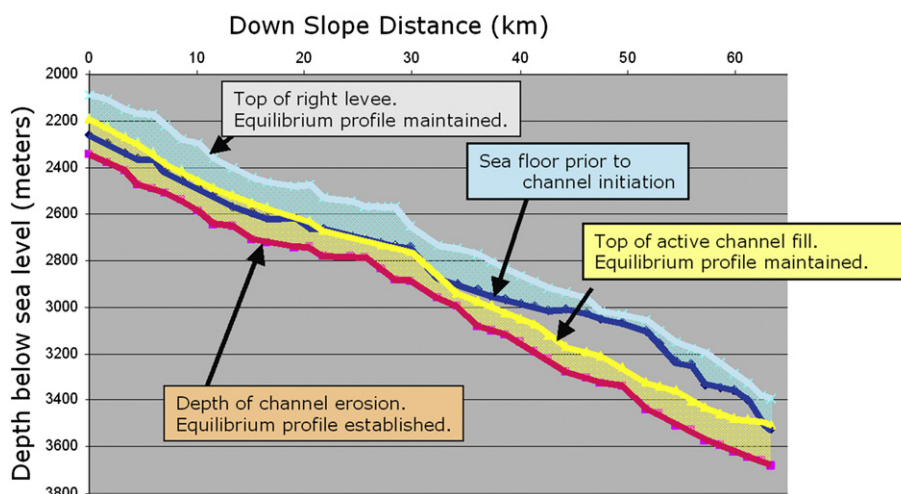


Fig. 4. Example dip profile along a near-seafloor channel-levee system from the continental slope of the Niger Delta that is well imaged by 3D seismic data for over 60 km down slope. The original bathymetry prior to channel initiation, indicated by the dark blue horizon, is determined by identifying the depth of the youngest horizon truncated by the channel system and downlapped by outer levees. The original surface is irregular, including a structurally elevated area near the distal end of the profile. The erosional base of the system is indicated by the red horizon. The top of active channel-fill (the top of high amplitude reflections in the system) is indicated by the yellow horizon; and the top of the right hand levee is indicated by the light blue horizon. Note that a nearly smooth profile is established immediately through erosion, despite significant irregularities on the initial seafloor profile. Elevated profiles after deposition within the channel system and on the levees are nearly parallel to the profile at the erosional base of the system.

decreasing density which allows deposition both within the channel conduit and in overbank settings of increasingly muddy sediments (Kneller, 2003; Labourdette, 2007; Wynn et al., 2007). Typically, an abrupt lateral shift of the channel position (avulsion) separates one cycle from the next (Sprague et al., 2002, 2005). Because most of the deposition takes place during the waning portion of the cycle compared to erosion during much of the waxing phase, each cycle will likely appear highly asymmetrical in the preserved stratigraphic record. The actual relative durations and amplitudes of the two phases are unknown.

6.2. Allogenic drivers

The driving mechanisms of flow energy cyclicity are unknown. In this paper, allogenic cyclicity is treated as the primary driving mechanism controlling waxing–waning cycles at all scales. In fact, allocyclicity may not control any of the cycles, but it is a convenient and simplifying assumption for modeling purposes that provides testable predictions. Several allogenic drivers, such as relative sea level, tectonism, and climate, likely influence turbidite architecture but the impact of one relative to another is unknown in most cases. Although autogenic processes presumably drive some of the changes that are manifest in turbidite channel deposits, they are poorly understood and difficult to use as a basis for making quantifiable predictions. If one wants to consider the effects of any particular autogenic process, it can be modeled within the cyclical allogenic framework either stochastically, or as a set of rules. It is useful to emphasize the cyclicity that is interpreted to result from allogenic mechanisms because these cycles are systematic, are easily modeled and will constrain predictions of the characteristics of turbidite deposits and their stacking pattern. Assumed allogenic cyclicity provides the basis for developing statistically definable trends that serve to constrain predictions, but presumably autogenic processes are responsible, at least in part, for the statistical spread that impacts the uncertainty of the predictions.

6.3. Cycle hierarchy

In most turbidite successions, at least three scales of waxing–waning cyclicity can be interpreted: element, complex set, and

sequence. The element scale of cyclicity is responsible for the erosion and filling of a single channel element. Likewise, the complex set scale of cyclicity results in the accumulation of a complex set and the sequence scale of cyclicity results in the accumulation of a sequence. We consider these three scales one at a time.

A sequence-scale cycle is the most familiar scale of waxing–waning cyclicity and the best documented (Posamentier and Vail, 1988; Posamentier et al., 1991; Mitchum et al., 1993). A sequence-scale cycle on the slope is expressed most completely by (1) a sequence boundary followed by (2) one or more complex set-scale cycles of potentially sand-rich sediments followed by (3) thin bedded siltstones of the lowstand wedge and then by (4) muddy deposits of the condensed section. Because the sequence scale of cyclicity has been described many times in detail, it will not be discussed here except to emphasize that the sequence in essence consists of a waxing phase, represented on the slope mostly by a stratigraphic surface, the sequence boundary, followed by increasingly muddy sediments deposited during a trend of waning energy.

A complex set-scale cycle is expressed by a series of channel elements that may be confined entirely or in part by an erosional valley, by levees, or by a combination of both. The stacking pattern of channel elements deposited during a complex set-scale cycle results in a succession of channel complexes that tend to follow a predictable pattern (Mutti, 1985; Mutti and Normark, 1987; McHargue, 1991; Mayall and Stewart, 2000; Peakall et al., 2000; Posamentier et al., 2000; Navarre et al., 2002; Sprague et al., 2002; Wynn et al., 2007). The erosional valley surface, if present, represents the waxing part of the complex set cycle in a high gradient setting. The early elements of the waning portion of the cycle strongly amalgamate because aggradation between elements is small in magnitude and the amount of lateral offset between elements is limited by the high relief confinement of erosional valley walls or levees. These amalgamated channel elements constitute an amalgamated channel complex. As flow energy continues to wane, the equilibrium profile begins to rise so that the rate of aggradation between elements increases and amalgamation decreases with time. Aggradation from one channel element to the next requires accumulation of overbank sediments (Mutti and Normark, 1991; Clark and Pickering, 1996; Kneller, 2003). Overbank sediments usually are mud-rich and an increasing rate of aggradation implies that the mud fraction increases relative to sand

as energy continues to wane (Kneller, 2003; Labourdette, 2007). The aggrading succession of channel elements constitutes a separate channel complex because the stacking pattern of these aggradational elements differs strongly from the highly amalgamated stacking pattern that underlies them. Typically, the rate of aggradation continues to increase (McHargue, 1991; Peakall et al., 2000; Posamentier et al., 2000) until the next complex set-scale cycle begins, usually marked by abandonment of the active complex due either to avulsion or the end of turbidite sedimentation.

An element-scale waxing–waning cycle is expressed by the cut and fill of a single channel element. On the slope, a channel element begins with waxing flow energy that causes increased erosion of the substrate associated with a lateral shift of the channel position, that is, avulsion. Sediments within turbidity flows pass through the channel conduit to be deposited far down slope, leaving very little sediment behind within the channel except possibly for pebbly bed load lags at the channel base or muddy remnants of the dilute tails of the flows (Gardner and Borer, 2000) that may line the channel margin (Fig. 1). Although these deposits, called bypass deposits, often are very muddy, they represent some of the highest energy flows of the channel element (Mutti and Normark, 1987; Hubbard et al., 2010). Continued waxing energy causes continued erosion and extensive sediment bypass until flow energy begins to wane. Therefore, at a single outcrop or in a subsurface core, the waxing portion of the channel element energy cycle may be represented solely by an erosional surface, possibly coated by bypass deposits. It is not until flow energy begins to wane that a channel element starts to fill with sandy sediments (Gardner and Borer, 2000). Early deposits of the channel-fill often are highly amalgamated near the axis of the channel and interbedded with draping, muddy, bypass deposits at the channel margin (Fig. 1) (Campion et al., 2000). At any single location, continued waning flow energy results in decreasing magnitude and extent of amalgamation upward within the channel as a smaller proportion of each flow bypasses that location and more of the flow is deposited. Therefore, as flow energy wanes, the rate of sediment aggradation increases and the focus of deposition shifts progressively toward the proximal part of the channel profile, a process referred to as backfilling (Gardner and Borer, 2000). This means that at any one location, sandy beds will tend to thicken upward through the sediment fill of a channel element as the focus of sedimentation approaches that location along the channel profile (Campion et al., 2000). However, because of extensive amalgamation at the channel axis the apparent, amalgamated bed thickness may be greater in the lower part of the axial channel-fill. Therefore, the upward increase of bed thickness often is best expressed at the channel margins (Fig. 1) (Campion et al., 2000). The upward increasing trend in aggradation rate and bed thickness is accompanied by decreasing scour relief, decreasing amalgamation, and increasing preservation of interbedded muddy deposits as well as the tops of sandstone beds. The next element cycle begins with abandonment of the old element due either to avulsion or the end of turbidite sedimentation.

6.4. Mass transport deposits

Mass transport deposits are an important component of many slope channel systems at multiple scales (Mayall and Stewart, 2000; Posamentier and Kolla, 2003; Mayall et al., 2006; Armitage et al., 2009). Although there is some evidence that slump and debris flow deposits are most common near the base of a channel system (Mayall and Stewart, 2000; Posamentier and Kolla, 2003; Mayall et al., 2006), we have excluded mass transport deposits from the discussion above because their presence and abundance is not reliably tied to cyclicity. We have chosen to consider mass transport deposits stochastically.

6.5. Avulsion

Avulsion is a critical process in the development of turbidite channel architecture (Kolla, 2007). Unfortunately, this complicated process is poorly understood. Here, we treat avulsion as being tied to the initiation of the waxing phase of an energy cycle. During the waning phase of the previous cycle, channel architecture, and especially the relief of channel confinement, is in equilibrium with relatively mud-rich, small and low energy flows. The initiation of the next energy cycle brings with it flows that are much sandier, more dense, and much more erosive. Therefore, the potential for avulsion is greater at this time than at any other time in the energy cycle. Alternatively, some avulsions may be independent of an energy cycle resulting from (1) exceptional, large, energetic, turbidity flows, (2) mass flow deposits, or (3) mass failure of a levee. The occurrence of these non-cyclical avulsions, in either time or space, cannot be predicted as yet and are modeled stochastically.

7. Confinement hierarchy

The channel elements of some turbidite channel systems are confined by a single set of levees. However, the morphology of many turbidite channel systems, especially when located on the continental slope, indicates that confinement of turbidity flows can occur at two scales which we will refer to as inner confinement and outer confinement (Fig. 5). Inner confinement, results from the combination of erosion and/or overbank aggradation at the margin of a channel element, sometimes referred to as an inner levee or as an internal levee (Hubscher et al., 1997; Deptuck et al., 2003; Kane and Hodgson, 2011). Outer confinement results from the combination of erosion and/or overbank aggradation at the scale of a complex set. Outer confinement may take the form of an erosional valley wall, an outer levee, or a combination of the two. Increased overbank aggradation has an important impact on the stacking pattern of channel elements, potentially by increasing the amount of both inner confinement and outer confinement.

In the early part of the waning phase of a complex set-scale energy cycle the flows are large and probably sand-rich relative to flows later in the cycle (Kneller, 2003; Labourdette, 2007). The aggradation rate of both the inner and outer confinements can be low, limited by insufficient mud (Fig. 5). In this case, we speculate that channel element relief is low and confined sediment tends to nearly fill each channel element. Because little relief remains unfilled when the next element-scale cycle begins, the abandoned channel element has little influence on the path taken by the subsequent channel element. The result is a disorganized stacking pattern (McHargue et al., *in press*) (Fig. 6). We expect that disorganized stacking is favored by sand-rich flows that yield low rates of overbank aggradation and high rates of filling, especially when the complex set-scale cycle is in the early portion of the waning phase.

Mud-rich flows provide the mud volume that drives high rates of aggradation of inner confinement. Importantly, if outer confinement is present, either as an outer levee or as an erosional valley wall, and has sufficient relief, it is reasonable to expect that the overbank sediments of the channel element will be deflected and contained by the outer confinement, thus further enhancing the rate of aggradation on the inner confinement. Aggradation of the inner confinement increases channel element relief and thereby increases the probability that the channel element will not completely fill prior to initiation of the next element-scale energy cycle. The unfilled channel relief (Fig. 5) has the potential to influence, or even capture, the energetic flows of the next waxing phase. If this occurs, the result is an organized stacking pattern (McHargue et al., *in press*), where the position and morphology of the subsequent channel element are strongly influenced by the position and morphology of the previous

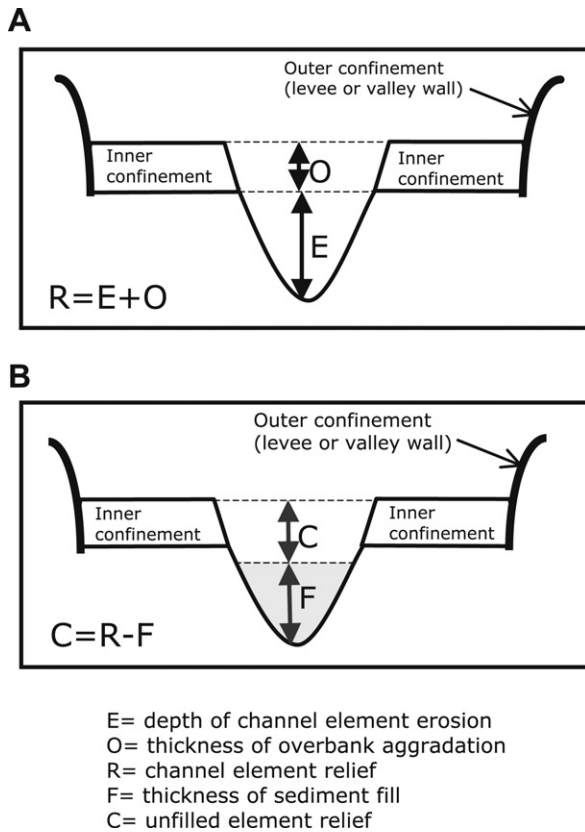


Fig. 5. A: Definition of channel element relief (R). Inner confinement is represented by an inner levee and outer confinement can be either an outer levee or an erosional valley wall. B: Definition of unfilled element relief (C).

element (Fig. 6). The second channel usually is offset by less than a channel width relative to the first channel (e.g. Posamentier et al., 2000; Posamentier and Kolla, 2003). We predict that mud-rich flows favor the development of organized stacking, because mud contributes most to the rate of overbank aggradation. Therefore, the probability of developing organized stacking increases as the complex set-scale waning phase progresses. The unfilled relief that is present when a channel element is abandoned presumably is filled by overbank sediments from the next younger channel (Piper et al., 1999). We expect the sediments that fill the abandoned channel relief to display an upward fining grain-size profile (Figs. 1 and 7). The decompacted thickness of the upward fining interval represents a minimum estimate of the unfilled relief of a channel at the time of its abandonment.

8. Autogenic drivers and patterns of architectural change down flow

8.1. Flow stripping, filtering, and scaling

Patterns of architectural change along a channel system are strongly influenced by autogenic drivers, especially flow stripping. When the top of a turbidity flow becomes elevated above channel confinement, then that unconfined portion of the flow spreads out, slows down and becomes detached from the underlying, confined portion of the flow. This process is called flow stripping (Piper and Normark, 1983; Peakall et al., 2000; Posamentier et al., 2000). It is the uppermost, mud-rich fraction of the flow that is preferentially removed by flow stripping, because turbidity flows are strongly density stratified, concentrated at the base and dilute at the top. Therefore, flow stripping is an effective filter that preferentially

removes fine-grained sediment from channelized turbidity currents. Flow stripping usually results in deposition of the fine-grained component in overbank positions which contributes to levee construction. Except for local variation, levee height tends to gradually decrease down flow (Skene et al., 2002; Pirmez and Imran, 2003; Posamentier and Kolla, 2003). Therefore, the channelized portion of the flow progressively loses its top to flow stripping and mud to the overbank while its relative sand concentration increases, a process we refer to as flow filtering. Flows can be thinner than the surrounding confinement, but they cannot remain thicker than confinement without the tops of the flows being stripped away. We refer to this effect as flow scaling; the height of the flow is scaled to the height of confinement.

Flow filtering tends to cause individual channelized flows to become thinner and sandier as they progress along their flow path. Flow scaling tends to constrain the upper limit of flow height of repeated channelized flows. Presumably, the effective longitudinal profile of the channel is in equilibrium with the time-averaged size and caliber of these scaled and filtered flows. Flow filtering is important for another reason as well. Flow filtering ensures that, as long as the upper part of a flow is clay-rich, overbank sediments are clay-rich. Clay-rich sediments are cohesive and characterized by moderate to high shear strength, making them relatively difficult to erode (Audet, 1998). Cohesive banks are necessary for bank stability and confinement, and without bank strength, channels with high sinuosity are not stable with time (Audet, 1998). As flows progress down slope, if gradient and levee height become progressively lower, the muddy upper portion of the stratified flows eventually will be completely stripped away and the lower, sand-rich portion of the flows will begin to spill onto the overbank. Near this point, the channel banks will be too sandy to be cohesive and the confinement height will be too low to be effective. We hypothesize that channels with non-cohesive, sandy banks tend to have low sinuosity and are unstable, avulsing frequently. The product is a weakly confined channel system, with laterally offset channels and sandy overbank with a low aggradation rate. Channel elements in this setting will be filled with sand-rich sediment and little if any recognizable abandonment deposits. Because of the low gradient and the low aggradation rate, each channel element will be thin.

9. Event-based approach to forward modeling

The observations, patterns, and hypotheses discussed thus far in this paper, some well constrained and some conjectural, can be expressed as mathematical statements which we refer to as rules. Rules are either empirical or predictive. Empirical rules are quantitative summaries of statistically defined patterns, relationships, or observed dimensions. Predictive rules generally are hypotheses regarding processes that are incompletely known. Rules are not independent. Interaction and feedback can produce complicated architectures from simple rules, as well as surprises which may require the improvement of existing rules, the development of new rules, or lead to new insights.

Single rules are of limited value by themselves for making quantitative predictions or quantitative characterizations of sparsely sampled channel systems. It is only when these rules are applied systematically in a forward modeling technique that their predictive value is optimized. We use an event-based (EB) forward modeling technique that facilitates the integration of geological information by constructing stochastic models as a sequence of depositional events (Pyrzc, 2004; Pyrcz et al., 2005; Pyrcz and Strebelle, 2006; Pyrcz et al., 2006; Pyrcz et al., in press). EB modeling is innovative in that it is (1) a forward model; (2) pseudo-process-based; (3) parameterized by flow axis centerlines and associated architectures; and (4) hierarchical. The EB forward modeling laboratory has the capability of

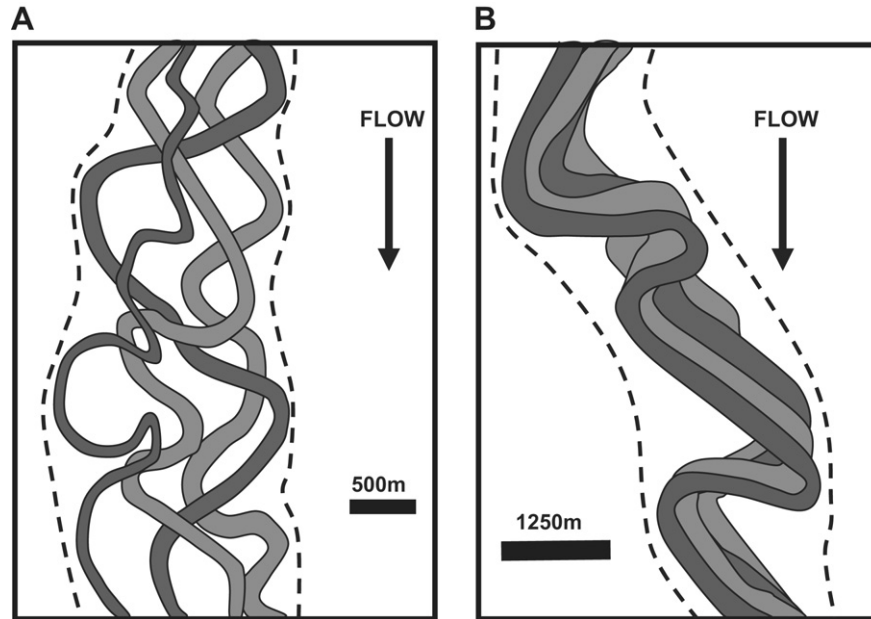


Fig. 6. Schematic examples in plan view of channel complexes illustrating contrasting stacking patterns of four channel elements. The location of outer confinement on either side of the channel complex is illustrated by a dashed line. A: Disorganized stacking pattern. The architecture and location of each element bears little resemblance to other elements. B: Organized stacking pattern with lateral offset of elements in a down-flow direction (arrow). The architecture and location of each element strongly resembles the previous element.

quickly constructing many realizations of channel systems that are consistent with the sparse constraints available from outcrop, seismic, or well control. From this suite of forward models, the range and probability of channel characteristics and their stacking patterns can be predicted quantitatively. After the experimental run, each realization of each model can be exhaustively analyzed to describe the genesis of each cell in the realization as well as property distributions and internal heterogeneities across each realization (Pyrzcz et al., 2005). The statistics from every realization of every acceptable model can be combined to address probability and uncertainty of properties and their spatial distribution.

We acknowledge that rule-based approaches to process modeling are less rigorous than physics-based approaches. However, physics-based processes are not adequately understood, the numerical methods are computationally intensive and resulting models often fail to reproduce high resolution architecture at

element scale. Rule-based models are able to: (1) use both empirical and predictive information summarized from partial analogs; (2) reproduce realistic architectures at element to complex set scales; and (3) generate a large number of model realizations rapidly (one realization of a model with several million cells in tens of seconds on a regular PC).

9.1. Boundary conditions for EB slope channel models

In the present form of EB forward modeling for slope channel models, the starting surface can be planar, channel-form, or irregular. The starting surface must be tilted basin-ward at a constant slope. The starting surface can be hypothetical or imported from constraining data such as a 3D seismic interpretation. Model dimensions usually are several tens of kilometers long, a few kilometers wide, and a few hundred meters thick. Individual turbidity currents are not modeled. Instead, each event consists of the net product of a single architectural element, erosion plus fill, constructed in response to the interaction of a set of rules. Element erosion and aggradation are controlled by rules that interact with energy cycles and substrate topography. The channel element is filled deterministically with axis, off-axis, and margin facies associations in proportions that are either constant or sampled from a distribution. The characteristics of each facies association are derived from local data or from a database of regional examples. Asymmetry of channel-fill is proportional to local curvature of the channel element. Subsequent channel elements may erode previous elements so that preserved channels and the preserved facies proportions of channel-fills can be substantially different from the original. For more detailed descriptions of the EB modeling method, the reader is referred to Refs. Pyrcz (2004), Pyrcz et al. (2005), Pyrcz and Strebelle (2006), Pyrcz et al. (2006), and Pyrcz et al. (in press).

10. Slope channel predictive model

Thus far, we have described the patterns, trends, and opinions that constitute many of the rules upon which the following models

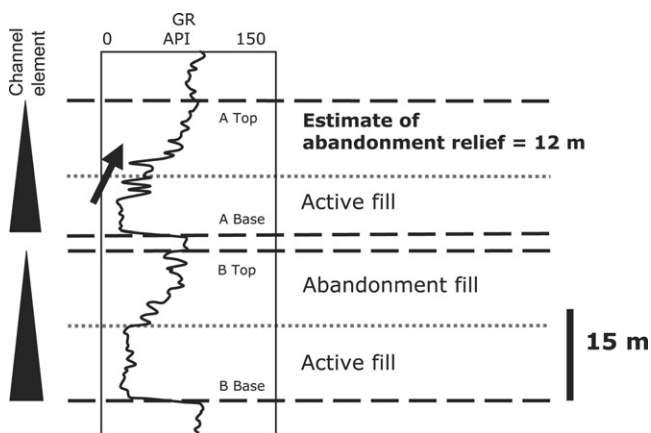


Fig. 7. Channel abandonment-fill overlying active channel-fill can be interpreted and the thickness can be estimated from well logs. Abandonment-fill is indicated by an upward increase in gamma ray values due to an upward increase in clay content and an upward decrease in sand bed thickness. In this synthetic example, the upper channel element, which is 21 m thick, consists of 9 m of active channel-fill overlain by 12 m of abandonment-fill. Although preserved in this example, underlying elements often are partially eroded so that abandonment-fill is partially or entirely removed.

are based. These models are crude, but they are a beginning, no better or worse than the rules. As experience and new data allow improvements in the rules, future models should improve as well. For example, initially, we were unable to generate an organized stacking pattern of channel elements in our EB models. Consequently, we hypothesized that unfilled relief of one channel element had the potential to confine the subsequent channel element and contribute to organized stacking (McHargue et al., *in press*). After incorporating this hypothesis as a rule, organized stacking formed in a logical manner, especially when rates of overbank aggradation were high. Furthermore, without the need of additional rules, down slope translation (sweep) of younger elements developed in complexes with organized stacking. This example of rule development emphasizes that an EB model is a hypothesis and illustrates an example emergent behavior that matches observations of natural systems. The EB model benefits from being conditioned by specific data sets in order to provide specific robust predictions for comparison to real world examples. When coded in a forward modeling package such as EB, the predictions are quantitative, 3D, reproducible and therefore testable.

We hypothesize that on the continental slope, the evolution of flow caliber toward an increasing proportion of mud during the waning phase of cycles at all scales tends to construct a channel complex set with a predictable succession of architectures. Aspects of this architectural succession have been noted previously (e.g. Stelting et al., 1985; Mutti, 1985; Phillips, 1987; McHargue, 1991; Pirmez and Flood, 1995; Clark and Pickering, 1996; Gardner and Borer, 2000; Mayall and Stewart, 2000; Navarre et al., 2002; Posamentier and Kolla, 2003; Cross et al., 2009). In different settings along a profile, or in systems with different flow calibers, the prominence of any stage can vary or even be absent although the stages are likely to occur in the following order: (1) erosion of a complex set-scale container; (2) accumulation of sand-rich, laterally offset, amalgamated channel elements with low rates of overbank aggradation; (3) development of channel elements with disorganized stacking and modest amalgamation as overbank aggradation begins to increase; and (4) establishment of under-filled channel elements with organized stacking as overbank sediments accumulate at a high rate (Fig. 8). As stated earlier, the relative prominence of each stage can vary considerably depending on local conditions, position along the slope profile, and the caliber of supplied sediment. Also, exceptions to this model are to be expected. The succession of stages can be interrupted by the initiation of a new complex set-scale cycle or truncated by erosion. These architectural stages and their implications in different settings and with different flow calibers are discussed here.

10.1. Mixed sand-mud system

The rules have been developed primarily to model turbidite channel systems on the continental slope in which the time-averaged flow caliber is rich in both sand and mud (mixed sand-mud systems) because these are important petroleum reservoirs. Some examples of channel systems that display all four stages are: Angola subsurface (Labourdette and Bez, 2010), the Joshua system of the Gulf of Mexico (Posamentier, 2003), De Soto area system (Posamentier and Kolla, 2003), Niger western slope (Deptuck et al., 2007), and western Amazon (Nakajima et al., 2009). The specific EB models illustrated in Fig. 8 are of mixed sand-mud turbidite channel systems on a moderately steep slope gradient (perhaps $>1^\circ$). For comparison, the hypothesized architectures on a low gradient will also be discussed. In addition, the hypothesized variations in architectures of sand-dominated and mud-dominated systems will be compared to the illustrated models. The illustrated EB models are for limited lengths, tens of kilometers, of channel

systems. This scale is sufficient to model the reservoirs of petroleum accumulations while eliminating the need for many rules to account for down-flow changes in flow parameters due either to changes in gradient or to evolving flow caliber (Fig. 3).

10.1.1. Stage 1, complex set-scale erosion (Fig. 8A)

Erosion initiates the development of a slope channel system on a moderate to high gradient. We assume that the slope channel system is eroded by many channel elements during the waxing phase of a complex set-scale cycle. These events are confined by inner confinement and the developing outer confinement as the equilibrium profile drops. During the waxing phase, the time-averaged flow caliber contains the highest proportion of sand and has the greatest erosive power. In response to these energetic conditions, the equilibrium profile falls through time, driving erosion. Except for clast-rich lags and fine-grained laminated mudstone from the tail of turbidity currents, sediment transported by these erosive flows bypasses the erosional valley to be deposited at some distal location where the gradient is low. A possible exception is the potential to preserve channel remnants of erosional terraces on the flank of the valley (Fig. 9).

10.1.2. Stage 2, amalgamation (Fig. 8B)

As the waxing phase gradually transitions to the early waning phase of the complex set-scale cycle, the equilibrium profile stabilizes and the slope channel system no longer deepens. Deposits of the coarsest components of the flows are preserved as bed load lags on the valley floor. The entire valley is draped with mud-rich deposits that represent the tails of bypassing flows, but these deposits might be preserved only on the flanks of the valley because subsequent flows are still energetic enough to re-erode them near the axis. In this early stage of sedimentation, the accumulation of mass transport deposits is common and occasionally voluminous. Although important components of the fill, mass transport deposits have not been included in the illustrated model (Fig. 8). As the waning phase progresses, the time-averaged flow caliber becomes slightly muddier and the equilibrium profile begins to slowly rise. Sediment bypass becomes less effective and increasingly, sand-rich deposits accumulate within the erosional confinement of each channel element. Some fine-grained sediments accumulate as overbank deposits within the valley but they are not often preserved, because, due to low rates of aggradation, subsequent avulsion and re-incision by younger elements rework these deposits and carry them farther down system. The resulting architecture is highly amalgamated, containing laterally offset channel elements. Overbank aggradation is very low and channel elements are filled with sand-rich sediments so inner confinement is ineffective and prominent avulsions result in disorganized stacking.

10.1.3. Stage 3, disorganized stacking (Fig. 8C)

As the waning energy phase progresses, the time-averaged caliber of repeated flows becomes increasingly muddy, the equilibrium profile rises and both the channel elements and their overbank deposits aggrade at an increasing rate. Increased aggradation requires deposition of increasing volumes of mud-rich sediments in overbank positions (inner confinements in Fig. 8) within the valley because successive channel elements cannot aggrade without aggradation of the overbank. Likewise, as the overbank aggradation component of confinement increases relative to the erosional component, channel amalgamation decreases and the volume of channel deposits decreases relative to the volume of overbank sediments. The potential for development and growth of outer improves at this time, but may be prevented if valley relief is too great to allow turbidites to overflow the valley

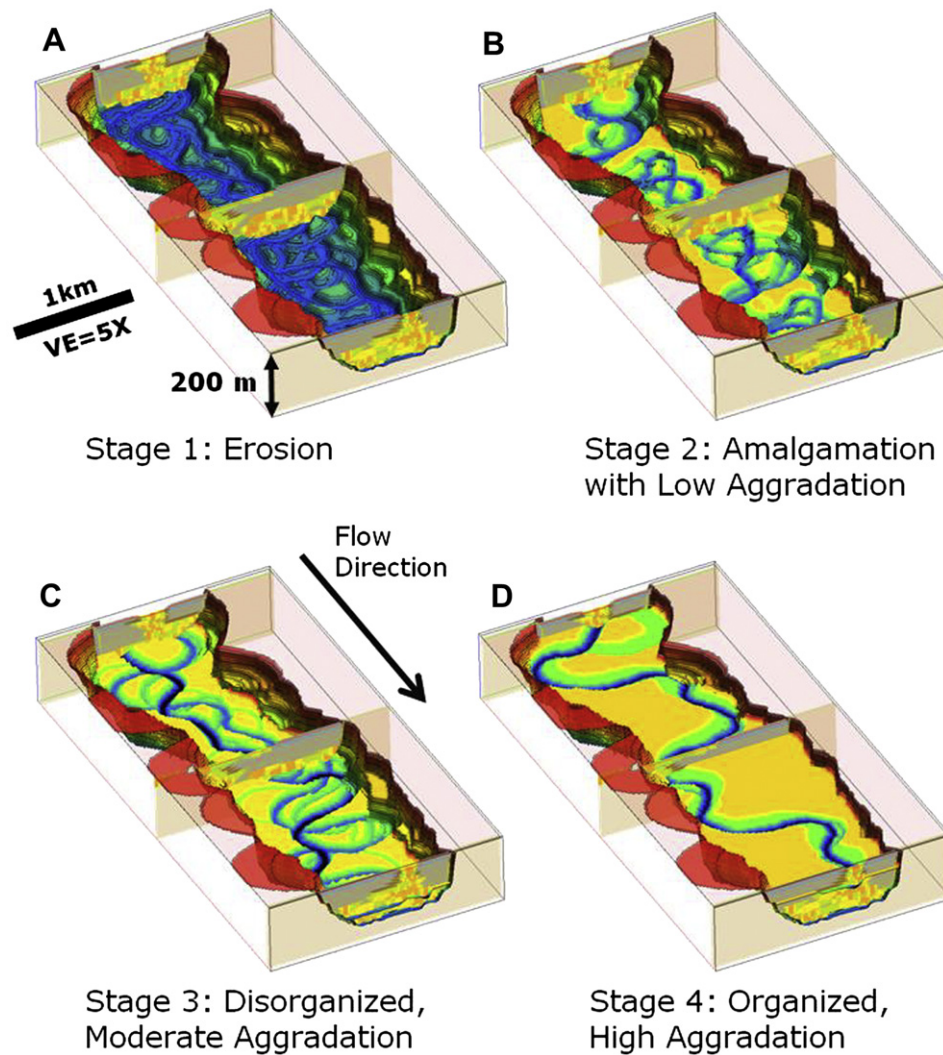


Fig. 8. Example event-based forward model showing 4 architectural stages. Each display shows the surface of a representative event (channel element plus overbank deposits) as preserved after erosion by younger events. The total accumulated sediments at the locations of three cross-sections are illustrated for reference. Depth of erosion of valley floor or walls = red (shallowest), yellow, green, and blue (deepest). Within valley-fill deposits as seen in plan view, yellow = overbank deposits of the selected event. The channel elements that erode the selected event are shown as blue (deep erosion) or green (shallow erosion). In the three cross-sections, all accumulated sediments at each of the three locations are illustrated. In the cross-sections, the facies associations of channel-fill are represented by orange (axis), yellow (off-axis), green (margin), and gray (abandonment). Overbank deposits are represented as gray. The model is 2 km × 10 km × 200 m. Vertical exaggeration = 5×. A: Stage 1 erosion. This figure shows the valley at maximum erosion without sediment fill. B: Stage 2 channel amalgamation with low rate of aggradation. C: Stage 3 Disorganized channel stacking pattern with moderate rate of aggradation. D: Stage 4 Organized channel stacking pattern with high rate of aggradation.

walls. If all of the overbank muds are confined by the valley walls, then the aggradation rate of inner confinement can be high and channel elements will not fill with sediments before the next element-scale energy cycle begins. Nevertheless, the under-filled relief of channel elements is insufficient to confine the flows of the next element-scale waxing phase which is marked by avulsion. As a result, channel elements stack in a disorganized pattern.

10.1.4. Stage 4, organized stacking (Fig. 8D)

As the waning energy phase continues to progress, the time-averaged caliber of repeated flows becomes even muddier, the equilibrium profile continues to rise and channel elements aggrade at an increasing rate along with their overbank deposits. The unfilled relief of under-filled channel elements increases because of the increasing contribution of overbank (inner confinement) aggradation to channel relief. The unfilled relief is now sufficient to confine the energetic waxing flows of the next

element-scale energy cycle. Organized stacking of channel elements results where each younger channel element is forced to follow near the path of the previous channel element (Figs. 6 and 9). Flow momentum focuses erosion of channel walls in a down-slope direction resulting in offset of successive elements (Fig. 10A). The increasing rate of overbank aggradation is associated with decreasing erosion during each element-scale waxing phase. Nevertheless, channel amalgamation increases, because the change from disorganized to organized stacking superimposes channel elements. In very muddy systems, extremely organized superimposes successive channel elements (Pirmez et al., 2000; Posamentier et al., 2000; Popescu et al., 2001; Posamentier, 2003; Posamentier and Kolla, 2003; Schwenk et al., 2005; Deptuck et al., 2007). Perhaps very muddy systems with turbidity currents of long duration are one situation that favors the development of lateral accretion with expanding meander loop radii, and high sinuosities similar to fluvial systems.

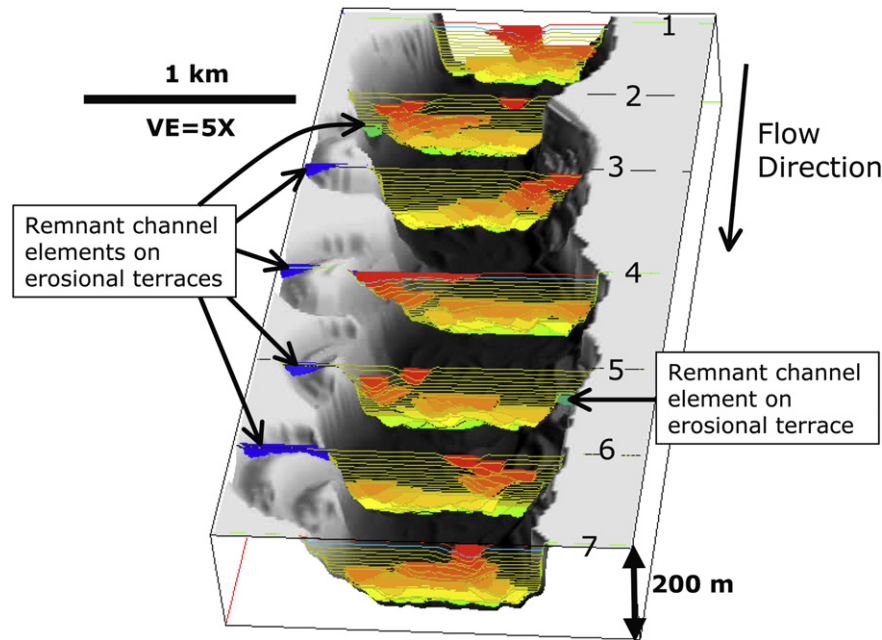


Fig. 9. Multiple cross-sections through EB model in Fig. 8. Each cross-section shows the channel elements and overbank deposits and their stacking pattern within the erosional valley container. The relative ages of channel elements are shown by color: blue (oldest) to green, yellow, orange, and red (youngest). Overbank deposits are transparent. Because of channel sinuosity, organized stacking is expressed locally in a variety of ways: vertical stacking, sections 1 and 7; persistent lateral offset, sections 3 (right) and 4 (left); a reversal of offset direction, section 6; and local, brief disruption of organized stacking, sections 2 and 5. Possible channel remnants on erosional terraces can be seen along the valley walls on sections 2 and 5 or at the top of the valley in sections 3–6. Vertical exaggeration = 5 \times .

Eventually, a new complex set-scale energy cycle begins with far more energetic sandy flows during the waxing phase. Complex set-scale avulsion is most likely at this time but if outer confinement is sufficiently high, either as unfilled erosional valley confinement or as high relief outer levees, the next complex set may be captured by the unfilled relief of the older complex set. This is most likely in proximal settings with deeply eroded slope channel systems on steep slopes.

10.2. Architectures on a low gradient

The same flows that produce the modeled architecture discussed above will produce very different architectures in distal areas of low gradient (perhaps 0.5° or less for mixed sand-rich and mud-rich systems). We hypothesize that stage 1 erosion will be minor or even absent. In stage 2, any erosional relief that is present will be occupied by amalgamated channel elements filled by sand-rich sediments (Fig. 1B). In stage 3 at this setting, the caliber of overbank sediment is critical in determining architecture. For example, the Makassar Strait system contains enough mud to build prominent levees at the base of slope (Posamentier et al., 2000; Posamentier and Kolla, 2003). The levees provide sufficient confinement with rapid aggradation to allow a channel stacking pattern that evolves through stages 1–4. However, rapid depletion of mud down flow, as a consequence of flow stripping, causes mixed sand-mud flows to evolve rapidly into sand-rich flows. In the distal Makassar system, as in other sand-rich systems in a low gradient setting, the mud that remains in the upper portion of the flows is deposited on the overbank. However, the levees are too small to confine multiple element cycles so avulsion between elements is likely and organized stacking of stage 4 cannot develop. If mud volume is insufficient to allow the development of effective cohesive banks, confinement is weak, the rate of overbank aggradation is very low, channel elements are thin, and stage 3 aggradation is slight to absent. Sand-rich sediments overfill most

channel elements, further contributing to a sand-rich overbank. The resulting architecture will be a weakly confined (stage 2) channel system in which frequent avulsion and channel instability are common. Examples include portions of the Ross formation (Sullivan et al., 2000; Elliott, 2000), the Ongeluk River section of the Tanqua Karoo (Sullivan et al., 2000), the distal portion of the Makassar Strait system (Posamentier et al., 2000; Posamentier and Kolla, 2003), and near surface features of the Niger slope (Adeogba et al., 2005).

10.3. Mud-dominated systems

We hypothesize that on a high gradient beyond the canyon mouth, systems with a time-averaged flow caliber that is mud-dominated may exhibit only small to moderate erosion during stage 1, if any (e.g., aggradational zone of the Indus Fan (McHargue and Webb, 1986)). In stage 2, inner confinements may be small and outer levees ineffective if flows are sufficiently sandy, allowing amalgamation of channel elements across a broad area. However, because of the great volumes of mud in the flows, moderate to high rates of muddy overbank aggradation quickly result in the development of effective inner and outer levee confinement with high rates of aggradation. The disorganized stacking of stage 3 may be very short lived or even absent, giving way rapidly to stage 4 organized stacking and highly under-filled channel elements. Because of the high rate of inner confinement aggradation, a special case of organized stacking, lateral accretion, may develop along with prominent swing of meander loops and very high sinuosities.

In a more distal setting, on a low slope gradient, we hypothesize that stage 1 erosion will be unlikely. Because the time-averaged flow caliber contains so much mud, both stages 2 and 3 can be short lived or even absent and channel elements may aggrade rapidly along with muddy levees. Stage 4 organized stacking of high sinuosity channel elements, possibly including lateral accretion, dominates the system almost from the start. Examples of mud-rich

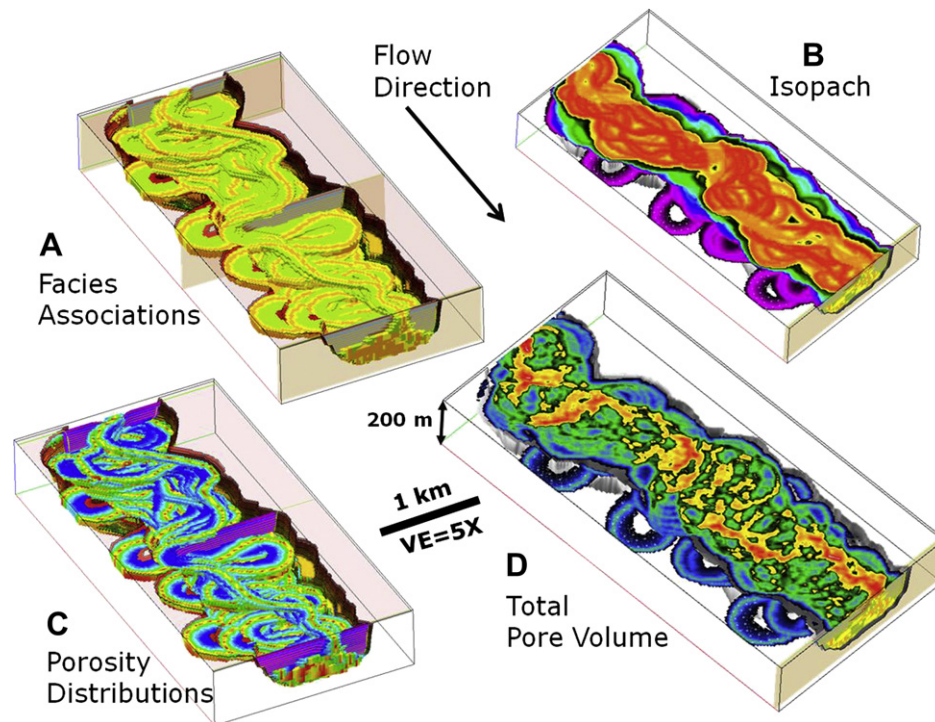


Fig. 10. Example quantitative products of the EB model in Fig. 8. A: 3D distribution of facies associations within channel elements. Axis = orange, off-axis = yellow, margin = green, abandonment and overbank deposits are transparent. Facies associations within any channel element can be asymmetrical in distribution at channel bends. The erosional surface of the valley walls is brown. B: Map of total sediment isopach superimposed on the valley model. Sediment thickness shown in red (thickest), yellow, green, blue, purple (thinnest). C: 3D volume of reservoir porosity based on statistical distributions for each facies association. Overbank deposits are transparent. Porosity within channel elements is indicated by red (highest porosity), yellow, light blue, dark blue (lowest porosity). The erosional surface of the valley walls is brown. D: Map of total reservoir pore volume superimposed on valley model. The total pore volume map represents the vertical summation of the thickness of each porosity value shown in C. Total pore volume for the model is indicated by red (highest pore volume), yellow, green, blue (lowest pore volume). Vertical exaggeration = 5×.

systems that display moderately to poorly developed architectures of stages 2 and 3 followed by prominent stage 4 organized stacking include the Amazon Fan (Pirmez et al., 2000), the Danube Fan (Popescu et al., 2001), and the Indus Fan (Schwenk et al., 2005). This architecture will persist distally until flow filtering removes most of the mud from the upper part of the flow so that overbank sediments are sufficiently sandy that outer levees are no longer cohesive. At this point, overbank deposits no longer effectively confine flows and channel positions and morphology are unstable. A weakly confined (stage 2) channel system develops consisting of rapidly avulsing, laterally offset channel elements. This zone of unstable, weakly confined channels will give way to a distributary system down flow and development of tabular sand bodies. This weakly confined to unconfined architecture may persist until the system is abandoned but if sufficient mud is introduced with time during the waning phase of the energy cycle, a channel-levee system may develop on top of the weakly confined to unconfined system containing architectures of stages 3 and 4.

10.4. Sand-dominated systems

We hypothesize that on a high gradient, systems with a time-averaged flow caliber that is sand-dominated may erode a high relief valley during stage 1 providing high relief outer confinement. During stage 2 amalgamation, channel elements aggrade slowly because sparse volumes of mud in the flows limit the rate of overbank aggradation. Element-scale erosion provides the only effective inner confinement for the sandy flows because sandy channel banks are non-cohesive and unstable. As a consequence, stage 2 channel amalgamation, perhaps including braided channel architectures, may dominate the entire system. Alternatively, if

sufficient clay is available in the late flows of the waning cycle, bank cohesion may develop, permitting the construction of disorganized stacking of filled channels (stage 3).

In a more distal low gradient setting, we hypothesize that in systems with a time-averaged flow caliber that is sand-dominated, stage 1 erosion may provide the only available outer confinement. As long as erosional outer confinement relief is effective, stage 2, laterally offset, amalgamated channel elements with low rates of aggradation and disorganized stacking fill the erosional outer confinement. Insufficient mud is available to allow formation of outer levees with appreciable relief so outer levees either are too small to effectively confine channel elements or levee confinement is short lived. Once the outer confinement is filled, avulsion allows channel elements to spread beyond the original boundaries of the erosional valley and a weakly confined channel system with rapidly avulsing, laterally offset channel elements develops. Further down flow, unconfined tabular sand bodies are deposited. An example of a sand-rich system with architectures of stages 1 and 2 in a proximal setting and stage 2 in a distal setting is located on the eastern margin of Corsica (Deptuck et al., 2008).

11. Discussion

We hypothesize that channel stacking patterns within a complex set-scale cycle tend to progress through a succession of architectural stages. These architectural stages are consistent with a suite of rules (observations, measurements, and hypotheses) for erosional slope channel systems on steep to moderate gradients with mixed sand-mud calibers. So, the architectural stages probably are best suited for constructing models of slope channel systems. Whereas some complex sets will display all of the four

stages, many complex sets will not. For example, some complex sets may be abandoned prior to development of stage 4 and the younger stages of some complex sets may be removed by the erosion from a younger complex set-scale cycle. Or, multiple complex sets with differing sediment calibers, different slope settings, or different aggradation rates may follow the same succession of stages but with changing proportions. We expect that stages 1–2 will dominate sand-rich complex sets whereas mud-rich levee-confined channel complex sets will be dominated by stages 2–4, or even 3–4. Lateral accretion is not included as part of the four architectural stages but we suspect that one favored setting for lateral accretion is late in the waning phase of a mud-rich complex set during stage 4 – organized stacking with high rates of aggradation of under-filled channel elements. Admittedly, there are channel complex sets with characteristics that appear to be inconsistent with the rules described here but we feel that these architectural stages serve as a useful standard for comparison.

The architectural stages and the rules from which they are derived are of limited value by themselves for making quantitative predictions or quantitative characterizations of sparsely sampled channel systems. The quantitative predictive power of rules is best exploited when rules are applied systematically in a forward event-based modeling package (McHargue et al., in press; Pyrcz et al., in press) to construct artificial 3D channel systems with realistic architectures (Figs. 8–10). Constructed models are dependent on the rules but are objective, reproducible and quantifiable and can be conditioned to available data. Interaction and feedback of simple rules can produce complicated architectures, such as the four stages, as well as surprises that may require the improvement of existing rules or the development of new rules. Multiple realizations and multiple alternative models can be constructed to quantitatively examine the probability of specific parameters of interest such as net volume, net-to-gross, connectivity, and tortuosity.

Examples of quantification are illustrated in Fig. 10. Examples include the 3D distribution of facies associations (Fig. 10A), a map of total sediment thickness within the slope channel system (Fig. 10B), the 3D distribution and quality of reservoir porosity (Fig. 10C), and a map of total reservoir pore volume (Fig. 10D). Furthermore, by running many models constructed with input values that span the entire reasonable range for each variable, a suite of possible models that are compatible with existing constraining data can be produced and statistically analyzed (Pyrcz et al., in press). The same models can be used to define probabilities for other specific attributes, such as pore volume, connectivity, and tortuosity.

12. Conclusions

- 1. Rules:** The study of many slope channel systems has led to the development of rules in the form of observations, measurements, and hypotheses. The rules were developed with the objective of constructing forward models of petroleum reservoirs in erosional slope channel systems on steep to moderate gradients with mixed sand-mud calibers. However, we anticipate that the rules are applicable to a broader range of slope channel systems.
- 2. Architectural hierarchy:** The consistent application of an architectural hierarchy is critical to organizing observations and measurements from diverse channel systems. In channelized systems, the fundamental architectural unit is the channel element, which consists of a channel-form surface and the sediments that fill it. Separate elements are distinguished from each other by an abrupt lateral offset of depositional facies. Multiple similar elements that stack in a consistent pattern can be grouped into a single complex, and, if multiple genetically related complexes are present, they can be grouped into

a single complex set. The term system is a general term used to refer to all of the genetically related channel components that are present in a single area regardless of hierarchy.

- 3. Facies associations:** Within a channel element, four facies associations are recognized: axis, off-axis, margin, and abandonment. In a relative sense, axis, off-axis, and margin differ from each other by the degree of amalgamation of beds and the relative abundance of sand, both of which are most common in the axis. The abandonment facies association overlies the other three facies associations in some channel elements and is characterized by an upward increase in mudstone interbeds.
- 4. Channel organization:** The thickness of the abandonment facies association is a basis for estimating the thickness of unfilled channel element relief at the time of channel abandonment. We hypothesize that low abandonment relief will have little influence on the location of the subsequent channel element and will result in a disorganized channel stacking pattern. Conversely, high abandonment relief can strongly influence the location of the subsequent channel element and will result in an organized channel stacking pattern in which the path of the younger channel element approximates the path of the former element.
- 5. Waxing–waning cyclicity:** We find it useful to interpret channelized turbidite deposits to be the product of multiple cycles of waxing flow energy followed by waning flow energy at multiple scales. Each cycle is interpreted to result from systematic changes in the volume and caliber of turbidity flows through time triggering first a fall of the equilibrium profile, which drives erosion and sediment bypass of the slope, followed by a rise of the equilibrium profile, which allows deposition on the slope of increasingly mud-rich sediments through time.
- 6. Cycle hierarchy:** In most turbidite successions, at least three scales of waxing–waning cyclicity can be interpreted: element, complex set, and sequence. The element scale of cyclicity is responsible for the erosion and aggradation of a single channel element. Likewise, the complex set scale of cyclicity results in the accumulation of a complex set, and the sequence scale of cyclicity results in the accumulation of a sequence.
- 7. Architectural stages:** The stacking pattern of channel elements within a complex set-scale cycle tends to be sequential: (1) erosion and sediment bypass; (2) amalgamation of channel elements associated with a low rate of aggradation; (3) a disorganized stacking pattern of channel elements associated with a moderate rate of aggradation; and (4) an organized stacking pattern of channel elements associated with a high rate of aggradation.
- 8. Variability of architectural stages:** Depending on variations in slope gradient, aggradation rate, and sediment caliber, the relative expression of the four stages will vary. For example, stages 1 and 2 may be absent or minor in mud-rich complex sets but prominent in sand-rich complex sets. Conversely, stage 4 may be prominent in mud-rich complex sets but absent in sand-rich complex sets. We hypothesize that organized stacking in particularly mud-rich complex sets may be one situation that favors the development of channel lateral accretion. We recognize that there are channel systems with characteristics that appear to be inconsistent with the sequence of architectural stages proposed here. Nevertheless, we expect that this model serves as a useful standard for comparison of diverse channel systems.
- 9. Event-based forward modeling:** Interaction and feedback of simple rules within the event-based forward modeling laboratory produces realistic architectures, such as the four stages described above. Multiple realizations and multiple alternative

models can be constructed to quantitatively examine the probability of specific parameters of interest.

Acknowledgements

The authors are grateful to Chevron Energy Technology Company for supporting the research and for providing permission to publish. Helpful reviews with suggestions for substantive improvements were provided by Drs. David Hodgson, Bill Morris, and Steve Hubbard, who are greatly appreciated.

References

- Abreu, V., Sullivan, M., Pirmez, C., Mohrig, D., 2003. Lateral accretion packages (LAPs): an important reservoir element in deep water sinuous channels. *Marine and Petroleum Geology* 20, 631–648.
- Adeogba, A.A., McHargue, T.R., Graham, S.A., 2005. Transient fan architecture and depositional controls from near-surface 3-D seismic data, Niger Delta continental slope. *American Association of Petroleum Geologists Bulletin* 89, 627–643.
- Armitage, D.A., Romans, B.W., Covault, J.A., Graham, S.A., 2009. The influence of mass-transport-deposit surface topography on the evolution of turbidite architecture: The Sierra Contreras, Tres Pasos Formation (Cretaceous), southern Chile. *Journal of Sedimentary Research* 79, 287–301.
- Audet, D.M., 1998. Mechanical properties of terrigenous muds from levee systems on the Amazon Fan. In: Stoker, M.S., Evans, D., Cramps, A. (Eds.), *Geological Processes on Continental Margins: Sedimentation, Mass-Wasting and Stability*, vol. 129. Geological Society of London, Special Publication, pp. 133–144.
- Beaubouef, R.T., Friedman, S.J., 2000. High-resolution seismic/sequence stratigraphic framework for the evolution of Pleistocene intra slope basins, Western Gulf of Mexico: depositional models and reservoir analogs. In: Weimer, P., Slatt, R.M., Coleman, J., Rosen, N.C., Nelson, H., Bouma, A.H., Styzen, M.J., Lawrence, D.T. (Eds.), *Deep-Water Reservoirs of The World*. Gulf Coast Section SEPM 20th Bob F. Perkins Research Conference, pp. 40–60.
- Bernhardt, A., Jobe, Z.R., Lowe, D.R., 2011. Stratigraphic evolution of a submarine channel-lobe complex system in a narrow. *Marine and Petroleum Geology* 28, 785–806.
- Campion, K.M., Sprague, A.R., Mohrig, D., Lovell, R.W., Drzewiecki, P.A., Sullivan, M.D., Ardill, J.A., Jensen, G.N., Sickafoose, D.K., 2000. Outcrop expression of confined channel complexes. In: Weimer, P., Slatt, R.M., Coleman, J., Rosen, N.C., Nelson, H., Bouma, A.H., Styzen, M.J., Lawrence, D.T. (Eds.), *Deep-Water Reservoirs of The World*. Gulf Coast Section SEPM 20th Bob F. Perkins Research Conference, pp. 127–150.
- Clark, J.D., Pickering, K.T., 1996. *Submarine Channels: Processes and Architecture*. Vallis Press, London, pp. 231.
- Cross, N.E., Cunningham, A., Cook, R.J., Taha, A., Esmail, E., El Swidan, N., 2009. Three-dimensional seismic geomorphology of a deep-water slope-channel system: the Sequoia field, offshore west Nile Delta, Egypt. *American Association of Petroleum Geologists Bulletin* 93, 1063–1086.
- Deptuck, M.E., Steffens, G.S., Barton, M., Pirmez, C., 2003. Architecture and evolution of upper fan channel-belts on the Niger Delta slope and in the Arabian Sea. *Marine and Petroleum Geology* 20, 649–676.
- Deptuck, M.E., Sylvester, Z., Pirmez, C., O'Byrne, C., 2007. Migration–aggradation history and 3-D seismic geomorphology of submarine channels in the Pleistocene Benin-major Canyon, western Niger Delta slope. *Marine and Petroleum Geology* 23, 406–433.
- Deptuck, M.E., Piper, D.J.W., Savoye, B., Gervais, A., 2008. Dimensions and architecture of late Pleistocene submarine lobes off the northern margin of Eastern Corsica. *Sedimentology* 55, 869–898.
- Elliott, T., 2000. Depositional architecture of a sand-rich, channelized turbidite system: The Upper Carboniferous Ross Sandstone Formation, western Ireland. In: Weimer, P., Slatt, R.M., Coleman, J., Rosen, N.C., Nelson, H., Bouma, A.H., Styzen, M.J., Lawrence, D.T. (Eds.), *Deep-Water Reservoirs of The World*. Gulf Coast Section SEPM 20th Bob F. Perkins Research Conference, pp. 342–373.
- Ferry, J.-N., Mulder, T., Parize, O., Raillard, S., 2005. Concept of equilibrium profile in deep-water turbidite systems: effects of local physiographic changes on the nature of sedimentary process and the geometries of deposits. In: Hodgson, D.M., Flint, S.S. (Eds.), *Submarine Slope Systems: Processes and Products*. Special Publication, vol. 244. Geological Society, London, pp. 181–193.
- Figueiredo, J.J.P., Hodgson, D.M., Flint, S.S., Kavanagh, J.P., 2010. Depositional environments and sequence stratigraphy of an exhumed Permian mudstone-dominated submarine slope succession, Karoo Basin, South Africa. *Journal of Sedimentary Research* 80, 97–118.
- Fildani, A., Hubbard, S.M., Romans, B.W., 2009. Stratigraphic evolution of deep-water architecture: Examples of controls and depositional styles from the Magallanes Basin. *SEPM Field Trip Guidebook*, southern Chile, 10, 73 pp.
- Flint, S.S., Hodgson, D.M., Sprague, A.R., Brunt, R.L., Van der Merwe, W.C., Figueiredo, J., Prélat, A., Box, D., Di Celma, C., Kavanagh, J.P., 2011. Depositional architecture and sequence stratigraphy of the Karoo basin floor to shelf edge succession, Laingsburg depocentre, South Africa. *Marine and Petroleum Geology* 28, 658–674.
- Gardner, M.H., Borer, J.M., 2000. Submarine channel architecture along a slope to basin profile, Brushy Canyon Formation, West Texas. In: Bouma, A.H., Stone, C.G. (Eds.), *Fine-Grained Turbidite Systems*. Memoir 72–American Association of Petroleum Geologists and Special Publication 68–SEPM, pp. 195–214.
- Hubbard, S.M., Fildani, A., Romans, B.W., Covault, J.A., McHargue, T.R., 2010. High-relief clinoform development: insights from outcrop, Magallanes Basin, Chile. *Journal of Sedimentary Research* 80, 357–375.
- Hubscher, C., Spiesz, V., Breitzke, M., Weber, M.E., 1997. The youngest channel levee system of the Bengal Fan: results from digital sediment echosounder data. *Marine Geology* 21, 125–145.
- Kane, I.A., Hodgson, D.M., 2011. Sedimentological criteria to differentiate submarine channel levee subenvironments: exhumed examples from the Rosario Fm. (Upper Cretaceous) of Baja California, Mexico, and the Fort Brown Fm. (Permian), Karoo Basin, S. Africa. *Marine and Petroleum Geology* 28, 807–823.
- Khan, Z.A., Arnott, R.W.C., 2011. Stratal attributes and evolution of asymmetric inner- and outer-bend levee deposits associated with an ancient deep-water channel-lobe complex within the Isaac Formation, southern Canada. *Marine and Petroleum Geology* 28, 824–842.
- Kneller, B., 2003. The influence of flow parameters on turbidite slope channel architecture. *Marine and Petroleum Geology* 20, 901–910.
- Kolla, V., 2007. A review of sinuous channel avulsion patterns in some major deep-sea fans and factors controlling them. *Marine and Petroleum Geology* 24, 450–469.
- Labourdet, R., 2007. Integrated three-dimensional modeling approach of stacked turbidite channels. *American Association of Petroleum Geologists Bulletin* 91, 1603–1618.
- Labourdet, R., Bez, M., 2010. Element migration in turbidite systems: random or systematic depositional processes? *American Association of Petroleum Geologists Bulletin* 94, 345–368.
- Mayall, M., Stewart, I., 2000. The architecture of turbidite slope channels. In: Weimer, P., Slatt, R.M., Coleman, J., Rosen, N.C., Nelson, H., Bouma, A.H., Styzen, M.J., Lawrence, D.T. (Eds.), *Deep-Water Reservoirs of The World*. Gulf Coast Section SEPM 20th Bob F. Perkins Research Conference, pp. 578–586.
- Mayall, M., Stewart, I., 2001. The architecture of turbidite slope channels. In: Fraser, S.I., Fraser, A.J., Johnson, H.D., Evans, A.M. (Eds.), *Petroleum Geology of Deep-water Depositional Systems, Advances in Understanding 3D Architecture*. The Geological Society Conference, March 20–22, 2001 Proceedings, Burlington House, Piccadilly, London. The Geological Society, unpaginated.
- Mayall, M., Jones, E., Casey, M., 2006. Turbidite reservoirs—key elements in facies prediction and effective development. *Marine and Petroleum Geology* 23, 821–841.
- McHargue, T.R., 1991. Seismic facies, processes, and evolution of Miocene inner fan channels, Indus Submarine Fan. In: Weimer, P., Link, M.H. (Eds.), *Seismic Facies and Sedimentary Processes of Submarine Fans and Turbidite Systems*. Springer Verlag, New York, pp. 403–413.
- McHargue, T.R., Pycroft, M.D., Sullivan, J.D., Clark, A., Fildani, B.W., Romans, J.A., Covault, J., Levy, H.W., Posamentier, H.W., in press. Event-based modeling of turbidite channel fill, channel stacking pattern, and net sand volume. *SEPM Special Publication*.
- McHargue, T.R., Webb, J.E., 1986. Internal geometry, seismic facies, and petroleum potential of canyons and inner fan channels of the Indus Submarine Fan. *American Association of Petroleum Geologists Bulletin* 70, 161–180.
- Mitchum, R.M. Jr., 1984. Seismic stratigraphic recognition criteria for submarine fans. *Gulf Coast Section SEPM Foundation Fifth Annual Research Conference*, pp. 63–85.
- Mitchum Jr., R.M., 1985. Seismic stratigraphic recognition of submarine fans. In: Berg, O.R., Woolverton, D.G. (Eds.), *Seismic Stratigraphy II*, vol. 39. American Association of Petroleum Geologists, pp. 117–136.
- Mitchum Jr., R.M., Sangree, J.B., Vail, P.R., Wornardt, W.W., 1993. Recognizing sequences and systems tracts from well logs, seismic data and biostratigraphy: examples from late Cenozoic. In: Weimer, P., Posamentier, H.W. (Eds.), *Siliclastic Sequence Stratigraphy: Recent Developments and Applications*, vol. 58. American Association of Petroleum Geologists, pp. 163–199.
- Mutti, E., 1985. Turbidite systems and their relation to depositional sequences. In: Zuffa, G.G. (Ed.), *Provenance of Arenites*. NATO-ASI series, Reidel, Dordrecht, Netherlands, pp. 65–93.
- Mutti, E., Normark, W.R., 1987. Comparing examples of modern and ancient turbidite systems: problems and concepts. In: Leggett, J.K., Zuffa, G.G. (Eds.), *Marine Clastic Sedimentology: Concepts and Case Studies*. Graham and Trotman, London, pp. 1–38.
- Mutti, E., Normark, W.R., 1991. An integrated approach to the study of turbidite systems. In: Weimer, P., Link, M.H. (Eds.), *Seismic Facies and Sedimentary Processes of Submarine Fans and Turbidite Systems*. Springer Verlag, New York, pp. 75–106.
- Nakajima, T., Peakall, J., McCaffrey, W.D., Paton, D.A., Thompson, P.J.P., 2009. Outer-bank bars: a new intra-channel architectural element within sinuous submarine slope channels. *Journal of Sedimentary Research* 79, 872–886.
- Navarre, J.-C., Claude, D., Libelle, E., Safa, P., Villon, G., Neskes, 2002. Deepwater turbidite system analysis, West Africa: sedimentary model and implications for reservoir model construction. *The Leading Edge* 21, 1132–1139.
- Peakall, J., McCaffrey, B., Kneller, B., 2000. A process model for the evolution, morphology, and architecture of sinuous submarine channels. *Journal of Sedimentary Research* 70, 434–448.

- Phillips, S., 1987. Dipmeter interpretation of turbidite-channel reservoir sandstones, Indian Draw Field, New Mexico. In: Tillman, R.W., Weber, K.J. (Eds.), *Reservoir Sedimentology*. Special Publication 40-SEPM, pp. 113–128.
- Piper, D.J.W., Normark, W.R., 1983. Turbidite depositional pattern and flow characteristics, Navy Submarine Fan, California Borderland. *Sedimentology* 30, 681–694.
- Piper, D.J.W., Hiscott, R.N., Normark, W.R., 1999. Outcrop-scale acoustic facies analysis and latest Quaternary development of Hueneme and Dume submarine fans, offshore California. *Sedimentology* 46, 47–78.
- Pirmez, C., Flood, R.D., 1995. Morphology and structure of Amazon channel. In: Flood, R.D., Piper, D.J.W., Klaus, A. (Eds.), *Proceedings of the Ocean Drilling Program, Initial Report*. Ocean Drilling Program, College Station, Texas, pp.23–45.
- Pirmez, C., Beaubouef, R.T., Friedman, S.J., Mohrig, D.C., 2000. Equilibrium profile and base level in submarine channels: examples from late Pleistocene systems and implications for the architecture of deepwater reservoirs. In: Weimer, P., Slatt, R.M., Coleman, J., Rosen, N.C., Nelson, H., Bouma, A.H., Styzen, M.J., Lawrence, D.T. (Eds.), *Deep-Water Reservoirs of The World*. Gulf Coast Section SEPM 20th Bob F. Perkins Research Conference, pp. 782–805.
- Pirmez, C., Imran, J., 2003. Reconstruction of turbidity currents in Amazon Channel. *Marine and Petroleum Geology* 20, 823–849.
- Popescu, I., Lericola, G., Panin, N., Wong, H.K., Droz, L., 2001. Late Quaternary channel avulsions on the Danube deep-sea fan, Black Sea. *Marine Geology* 179, 25–37.
- Posamentier, H.W., Vail, P.R., 1988. Eustatic controls on clastic deposition II – sequence and systems tract models. *Special Publication 42 – SEPM*, pp. 125–154.
- Posamentier, H.W., Erskine, R.E., Mitchum Jr., R.M., 1991. Models for submarine fan deposition within a sequence stratigraphic framework. In: Weimer, P., Link, M.H. (Eds.), *Seismic Facies and Sedimentary Processes of Submarine Fans and Turbidite Systems*. Springer-Verlag, New York, pp. 127–136.
- Posamentier, H.W., Meizarwan, Wisman, P.S., Plawman, T., 2000. Deep water depositional systems – Ultra-deep Makassar Strait, Indonesia. In: Weimer, P., Slatt, R.M., Coleman, J., Rosen, N.C., Nelson, H., Bouma, A.H., Styzen, M.J., Lawrence, D.T. (Eds.), *Deep-Water Reservoirs of The World*. Gulf Coast Section SEPM 20th Bob F. Perkins Research Conference, pp. 806–816.
- Posamentier, H.W., 2003. Depositional elements associated with a basin floor channel-levee system: case study from the Gulf of Mexico. *Marine and Petroleum Geology* 20, 677–690.
- Posamentier, H.W., Kolla, V., 2003. Seismic geomorphology and stratigraphy of depositional elements in deep-water settings. *Journal of Sedimentary Research* 73, 367–388.
- Prather, B.E., Booth, J.R., Steffens, G.S., Craig, P.A., 1998. Classification, lithologic calibration, and stratigraphic succession of seismic facies in intraslope basins, deep-water Gulf of Mexico. *American Association of Petroleum Geologists Bulletin* 82, 701–728.
- Prather, B.E., Keller, F.B., Chapin, M.A., 2000. Hierarchy of deep-water architectural elements with reference to seismic resolution: implications for reservoir prediction and modeling depositional systems. In: Weimer, P., Slatt, R.M., Coleman, J., Rosen, N.C., Nelson, H., Bouma, A.H., Styzen, M.J., Lawrence, D.T. (Eds.), *Deep-Water Reservoirs of The World*. Gulf Coast Section SEPM 20th Bob F. Perkins Research Conference, pp. 817–835.
- Pyles, D.R., Jennette, D.C., Tomasso, M., Beaubouef, R.T., Rossen, C., 2010. Concepts learned from a 3D outcrop of a sinuous slope channel complex: Beacon Channel complex, Brushy Canyon Formation, West Texas, U.S.A. *Journal of Sedimentary Research* 80, 67–96.
- Pyrzc, M.J., 2004. Integration of geologic information into geostatistical models. Unpublished Ph.D. Dissertation, University of Alberta, Edmonton, Canada, 250 p.
- Pyrzc, M.J., Deutsch, C.V., 2005. Conditional event-based simulation. In: Leuangthong, O., Deutsch, C.V. (Eds.), *Geostatistics Banff 2004*. Springer, New York, pp. 135–144.
- Pyrzc, M.J., Catuneanu, O., Deutsch, C.V., 2005. Stochastic surface-based modeling of turbidite lobes. *American Association of Petroleum Geologists Bulletin* 89, 177–191.
- Pyrzc, M.J., Sullivan, M., Drinkwater, N., Clark, J., Fildani, A., Sullivan, M., 2006. Event-based models as a numerical laboratory for testing sedimentological rules associated with deepwater sheets. *Gulf Coast Section SEPM 26th Bob F. Perkins Research Conference*, pp. 923–950.
- Pyrzc, M.J., Strebelle, S., 2006. Event-based geostatistical modeling of deepwater systems. *Gulf Coast Section SEPM 26th Bob F. Perkins Research Conference*, pp. 893–922.
- Pyrzc, M.J., McHargue, T.R., Clark, J., Sullivan, M., Drinkwater, N., Fildani, A., Posamentier, H., Romans, B., Levy, M., in press. Numerical modeling of deepwater channel stacking pattern from outcrop and the quantification of reservoir significance. *SEPM Special Publication*.
- Reading, H.G., Richards, M., 1994. Turbidite systems in deep-water basin margins classified by grain size and feeder system. *American Association of Petroleum Geologists Bulletin* 78, 792–822.
- Romans, B.W., Fildani, A., Hubbard, S.M., Covault, J.A., Fosdick, J.C., Graham, S.A., 2011. Evolution Of Deep-Water Stratigraphic Architecture, Magallanes Basin, Chile. *Marine and Petroleum Geology* 28, 612–628.
- Samuel, A., Kneller, B., Ralan, S., Sharp, A., Parsons, C., 2003. Prolific deep-marine slope channels of the Nile Delta, Egypt. *American Association of Petroleum Geologists Bulletin* 87, 541–560.
- Schwenk, T., Spieß, V., Breitzke, M., Hubscher, C., 2005. The architecture and evolution of the Middle Bengal Fan in vicinity of the active channel-levee system imaged by high-resolution seismic data. *Marine and Petroleum Geology* 22, 637–656.
- Skene, K.I., Piper, D.J.W., Hill, P.S., 2002. Quantitative analysis of variations in depositional sequence thickness from submarine channel levees. *Sedimentology* 49, 1411–1430.
- Sprague, A.R., Sullivan, M.D., Campion, K.M., Jensen, G.N., Goulding, D.K., Sickafoose, D.K., Jennette, D.C., 2002. The physical stratigraphy of deep-water strata: a hierarchical approach to the analysis of genetically related elements for improved reservoir prediction. *American Association of Petroleum Geologists Annual Meeting abstracts*, Houston, Texas, pp. 10–13.
- Sprague, A.R.G., Garfield, T.R., Goulding, F.J., Beaubouef, R.T., Sullivan, M.D., Rossen, C., Campion, K.M., Sickafoose, D.K., Abreu, V., Schellpeper, M.E., Jensen, G.N., Jennette, D.C., Pirmez, C., Dixon, B.T., Ying, D., Ardill, J., Mohrig, D.C., Porter, M.L., Farrell, M.E., Mellere, D., 2005. Integrated slope channel depositional models: the key to successful prediction of reservoir presence and quality in offshore West Africa. *CIPM, cuarto E-Exitop 2005*, February 20–23, 2005, Veracruz, Mexico, pp. 1–13.
- Stelling, C.E., Pickering, K.T., Bouma, A.H., Coleman, J.M., Cremer, M., Droz, L., Wright Meyer, A.A., Normark, W.R., O'Connell, S., Stow, D.A.V., DSDP Leg 96 Shipboard Scientists, 1985. Drilling results on the middle Mississippi Fan. In: Bouma, A.H., Normark, W.R., Barnes, N.E. (Eds.), *Submarine Fans and Related Turbidite Systems*. Springer, New York, pp. 275–282.
- Sullivan, M.D., Jensen, G.N., Goulding, F.J., Jennette, D.C., Foreman, J.L., Stern, D., 2000. Architectural analysis of deep-water outcrops: Implications for exploration and production of the Diana Sub-basin, western Gulf of Mexico. In: Weimer, P., Slatt, R.M., Coleman, J., Rosen, N.C., Nelson, H., Bouma, A.H., Styzen, M.J., Lawrence, D.T. (Eds.), *Deep-Water Reservoirs of The World*. Gulf Coast Section SEPM 20th Bob F. Perkins Research Conference, pp. 1010–1032.
- Sylvester, Z., Pirmez, C., Cantelli, A., 2011. A model of submarine channel-levee evolution based on channel trajectories: Implications for stratigraphic architecture. *Marine and Petroleum Geology* 28, 716–717.
- Weimer, P., Slatt, R.M., Coleman, J., Rosen, N.C., Nelson, H., Bouma, A.H., Styzen, M.J., Lawrence, D.T. (Eds.), 2000. *Deep-Water Reservoirs of The World*. Gulf Coast Section SEPM 20th Bob F. Perkins Research Conference.
- Winker, C.D., 1996. High-resolution seismic stratigraphy of a Late Pleistocene submarine fan ponded by salt-withdrawal mini-basins on the Gulf of Mexico continental slope. *Offshore Technology Conference Proceedings*, OTC 8024, 619–628.
- Wynn, R.B., Cronin, B.T., Peakall, J., 2007. Sinuous deep-water channels: genesis, geometry and architecture. *Marine and Petroleum Geology* 24, 341–387.